

On the spectrum of atmospheric motions

The Horizontal Spectrum of Vertical Velocities near the Tropopause from Global to Gravity Wave and Kolmogorov Scales

Ulrich Schumann

With contributions of Thomas Birner, Martina Bramberger, George Craig, Andreas Dörnbrack, Joseph Egger, Andreas Giez, Sonja Gisinger, Jörgen Jensen, Chris Kruse, Qiang Li, Erik Lindborg, Markus Rapp, Andreas Schäfler, Tobias Selz, Robert Sharman, Nils Wedi,

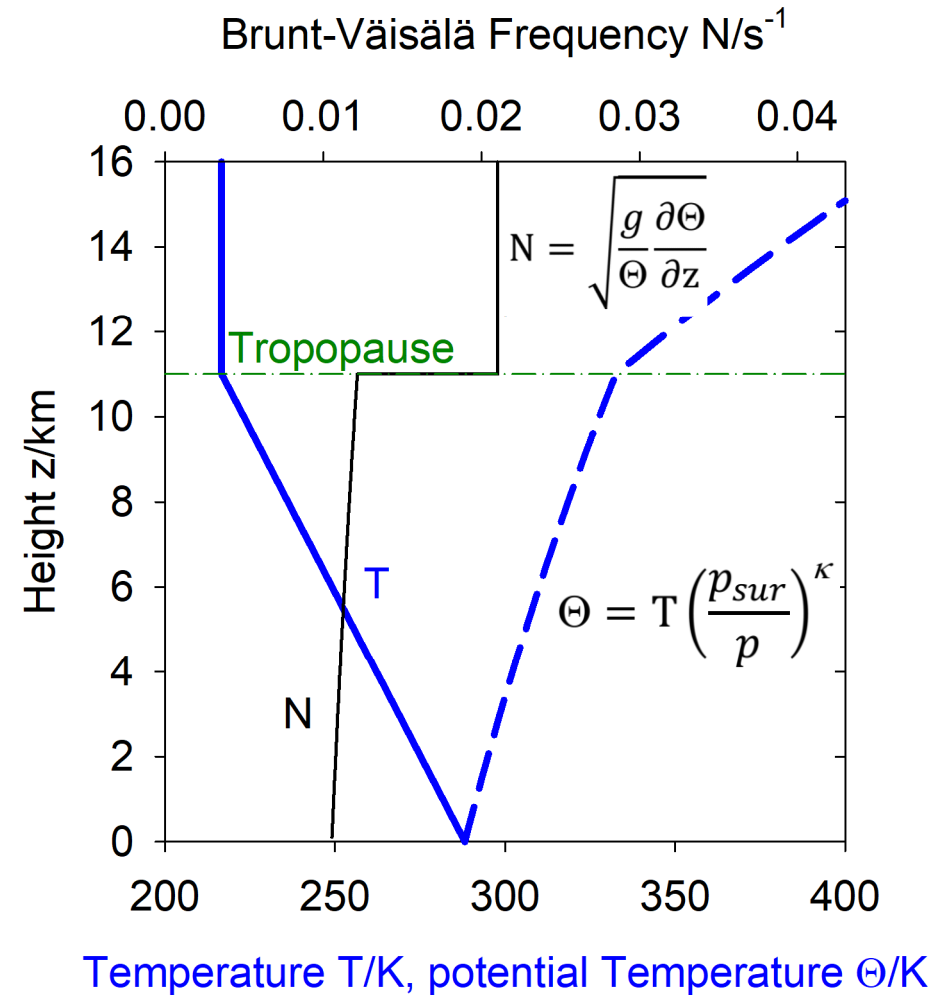
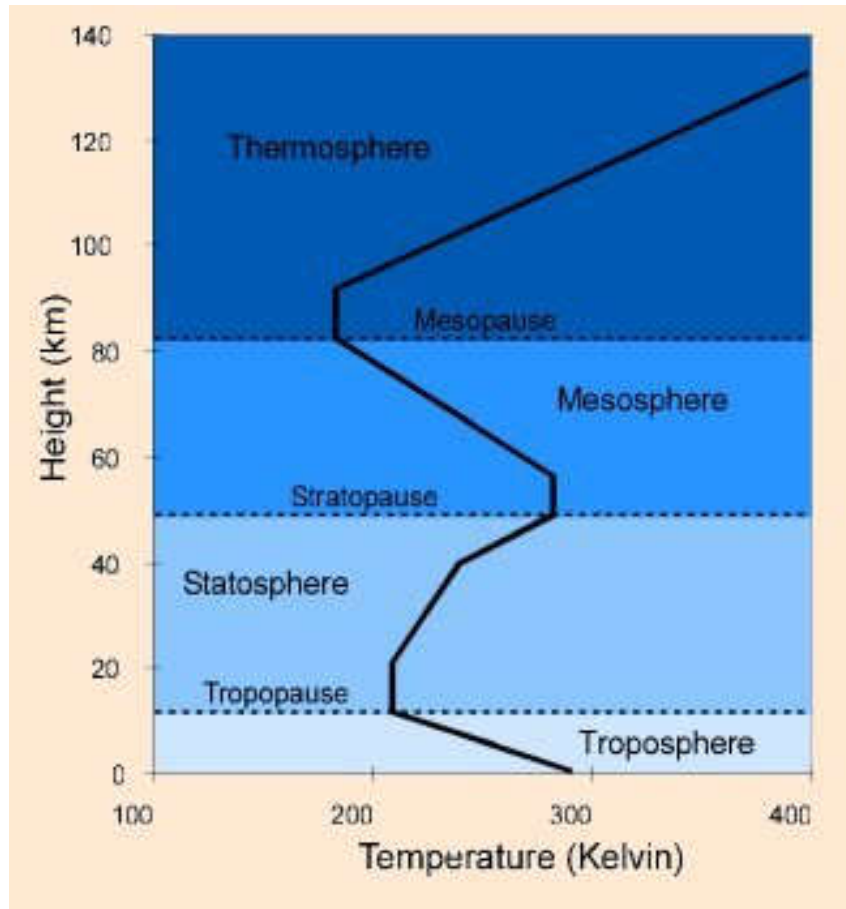
the DEEPWAVE and NAWDEX teams

and Michael Eckert and Jessika Wichner



Atmospheric Dynamics as an application of Fluid Mechanics

The stably stratified atmosphere, below and above the tropopause



Ludwig-Prandtl – Memorial Lecture # 63



1 (1957): Albert Betz, Göttingen

4 (1969): Ernst Schmidt, TU München

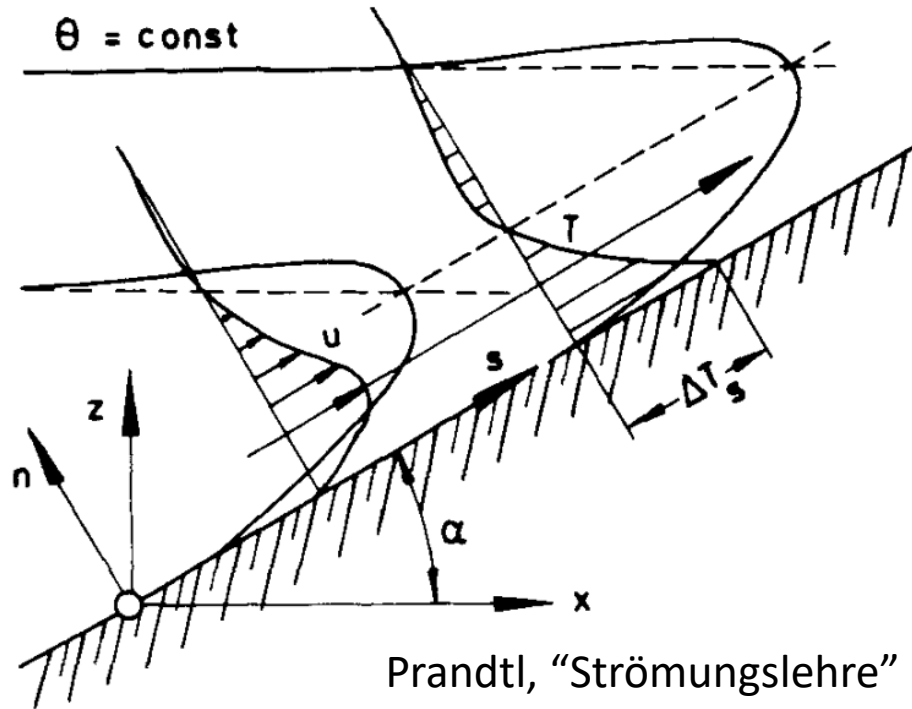
21 (1978): Jürgen Zierp, Karlsruhe

49 (2006): Rainer Friedrich, TU München

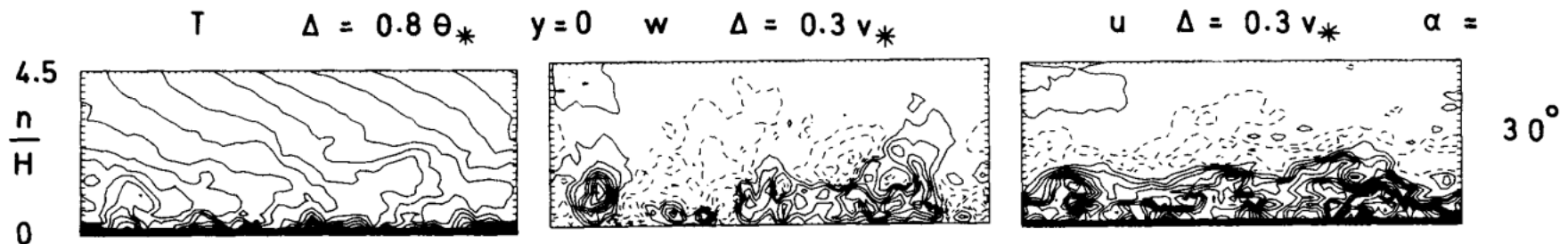
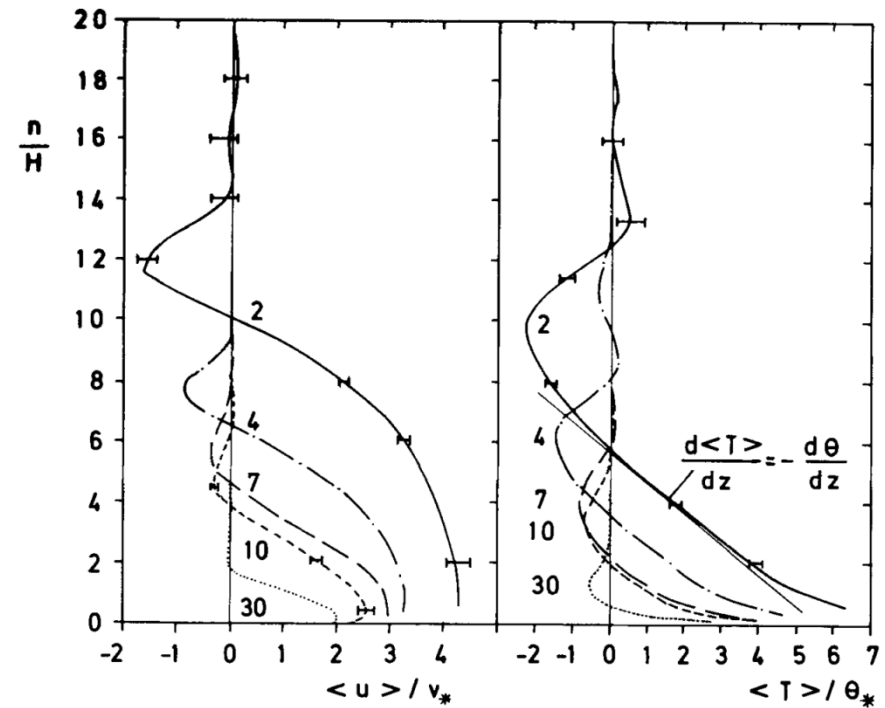
LES of Prandtl's slope boundary layer

646

U. SCHUMANN

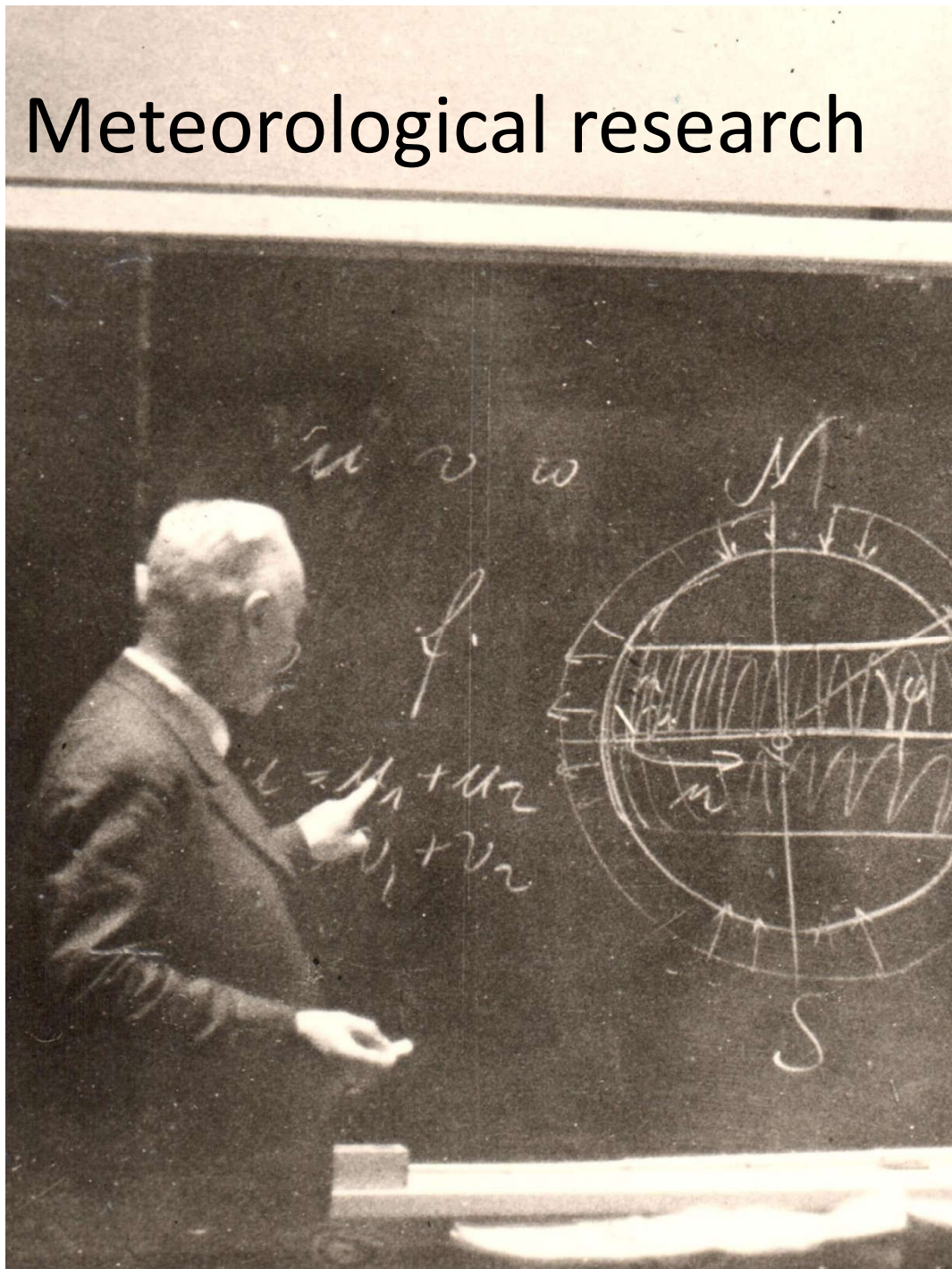


Prandtl, "Strömungslehre" (1942)



Schumann, Quart. J. Roy. Met. Soc. (1990) ⁴

Meteorological research



“a suitable occupation during peace”

(1945, cited from Eckert, 2019)

Turbulent Boundary Layer

Turbulent kinetic energy

Slope wind

Rotating flows, $f=2 \omega \sin(\varphi)$

Vorticity conservation

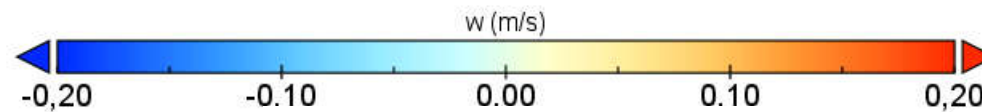
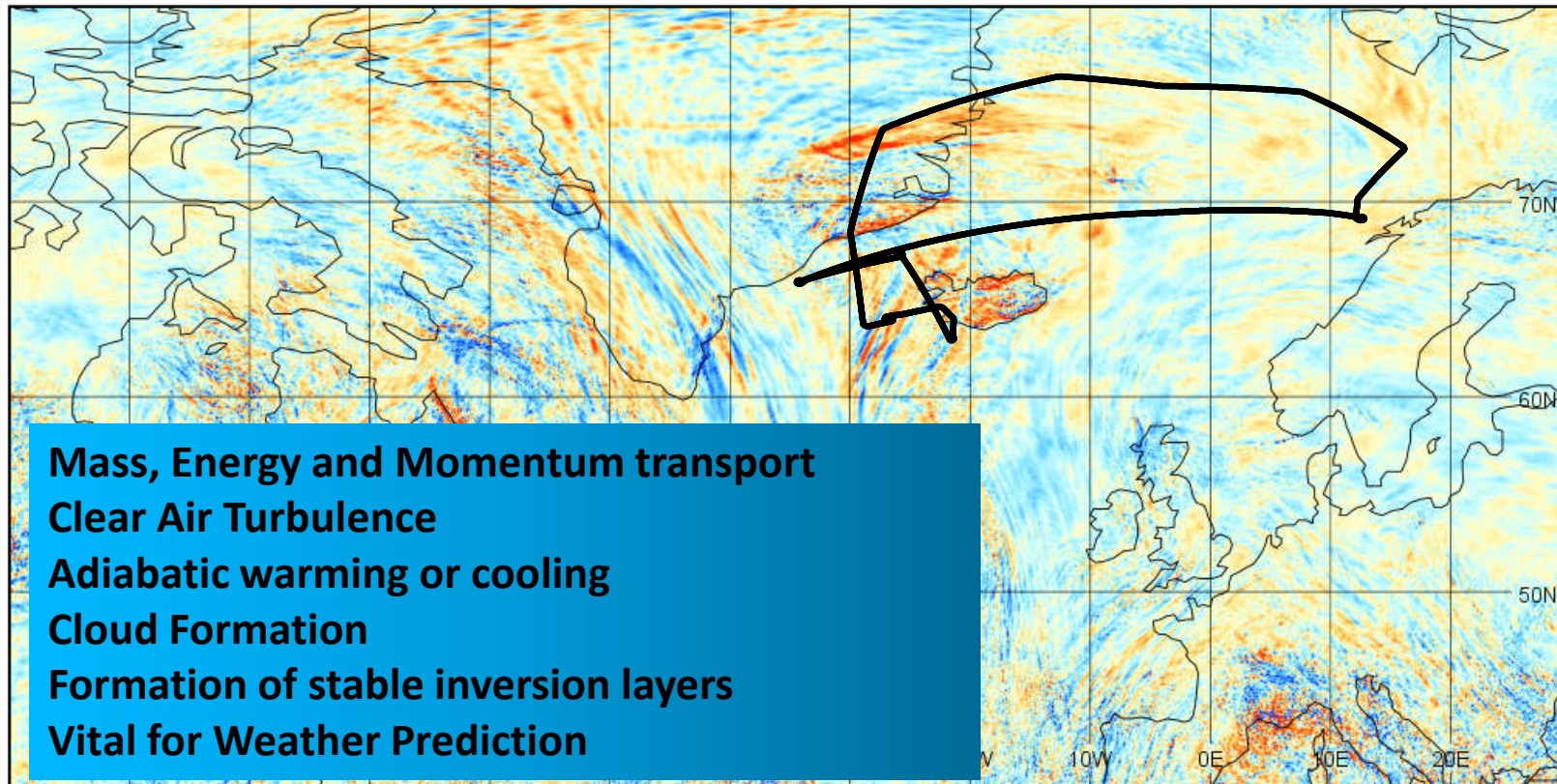
Weather Prediction

Vertical velocity (w) – Fundamental for Atmospheric Dynamics

$p=200$ hPa (≈ 12 km), 12 UTC 13 Oct 2016

HALO during NAWDEX

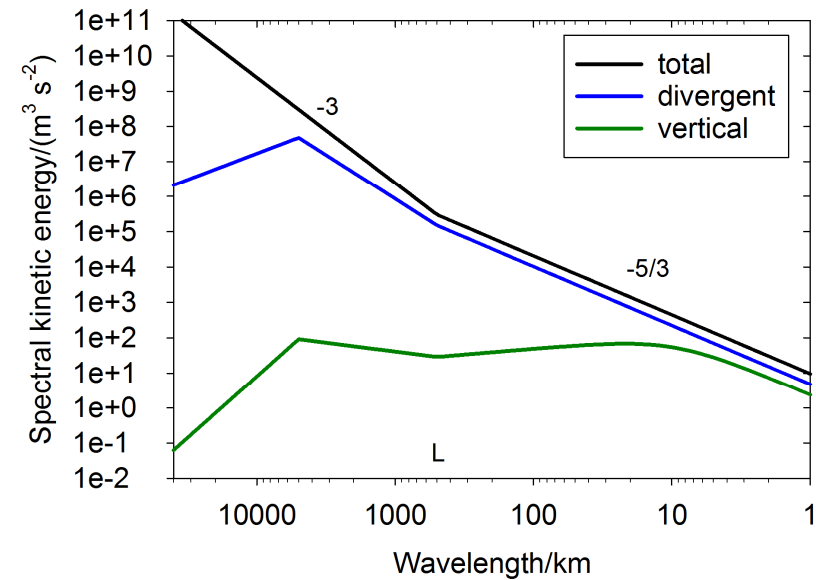
w



min=-1.3 m/s, max=1.5 m/s

10 to 100 times
smaller than
horizontal wind

ECMWF-IFS TCo7999 (Nils Wedi), 1.2 km grid resolution



1. What do we know about spectra of horizontal velocities (h-spectrum)
2. What do we know about spectra of vertical velocities (w-spectrum)
3. A hypothesis relating w-spectra with h-spectra
4. Validation
5. Implications
6. Conclusions

What do we know about spectra of horizontal velocities: from long-distance commercial aircraft data

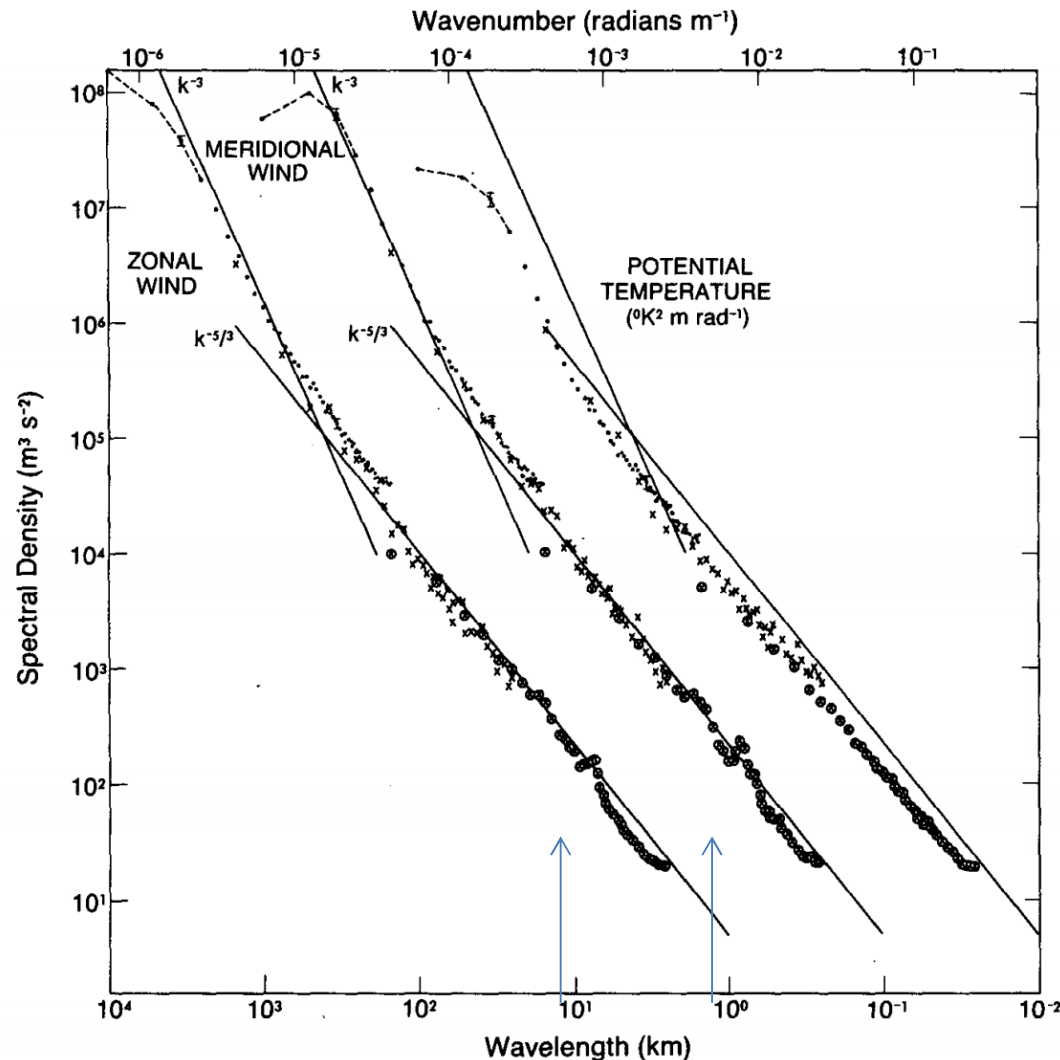


FIG. 3. Variance power spectra of wind and potential temperature near the tropopause from GASP aircraft data. The spectra for meridional wind and temperature are shifted one and two decades to the right, respectively; lines with slopes -3 and $-5/3$ are entered at the same relative coordinates for each variable for comparison.

Nastrom & Gage
(1985)

GASP: Global
Atmospheric
Sampling Program

6000 flights
B747 airliners,
Prandtl's pitot pipe
(TAS) and heading,
9–13 km altitude
at horizontal scales
of 2.6 to 10000 km

The “Canonical Spectrum” (Skamarock et al., 2014) of horizontal velocities from long-distance commercial aircraft data

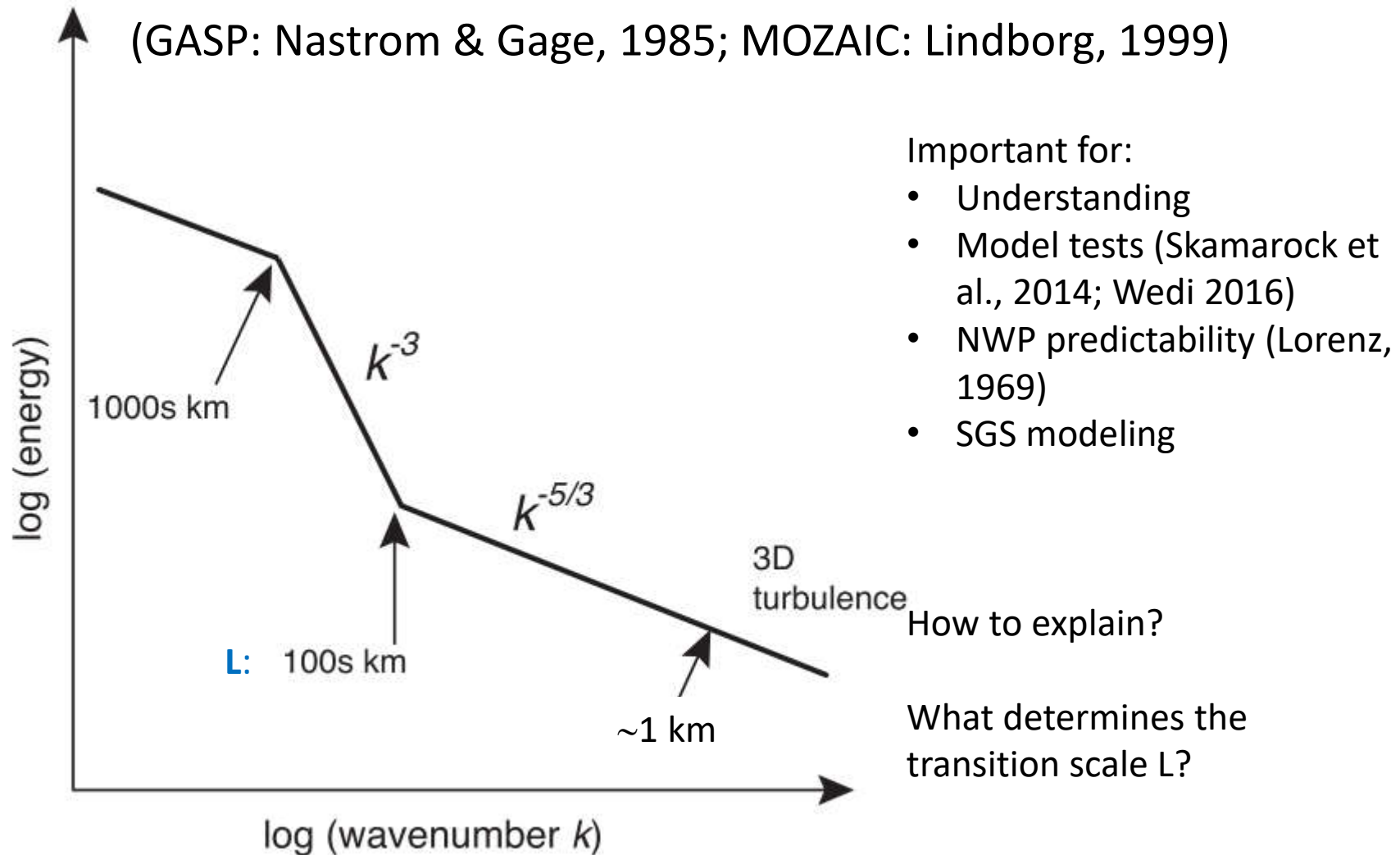


FIG. 1. Schematic of canonical atmospheric kinetic energy spectra.

Large-scale k^{-3} spectrum: Quasi-geostrophic turbulence (Charney, 1971)

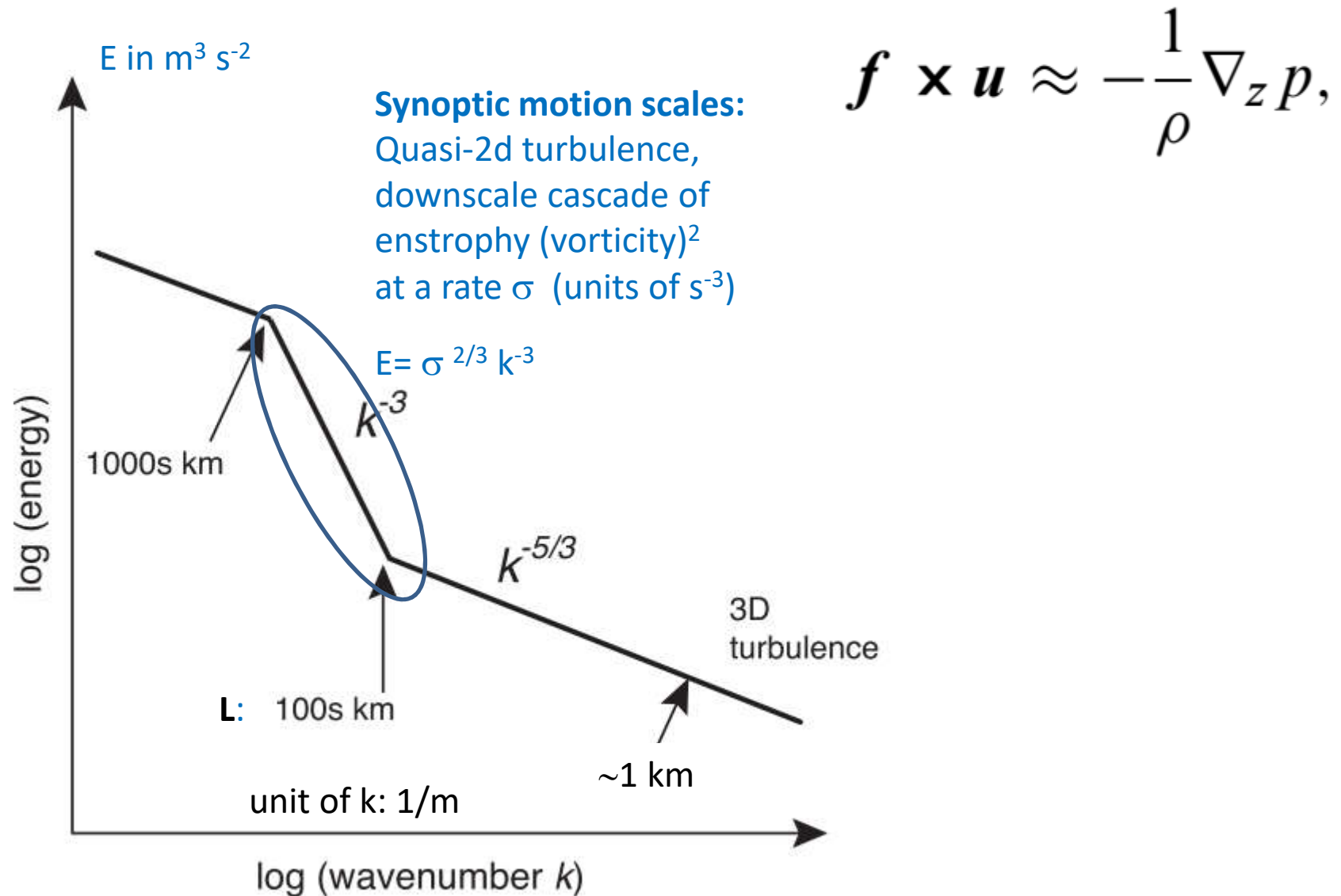
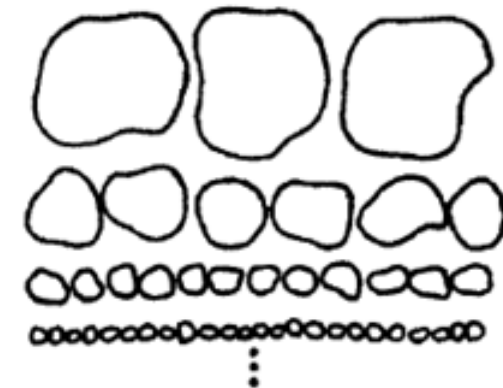
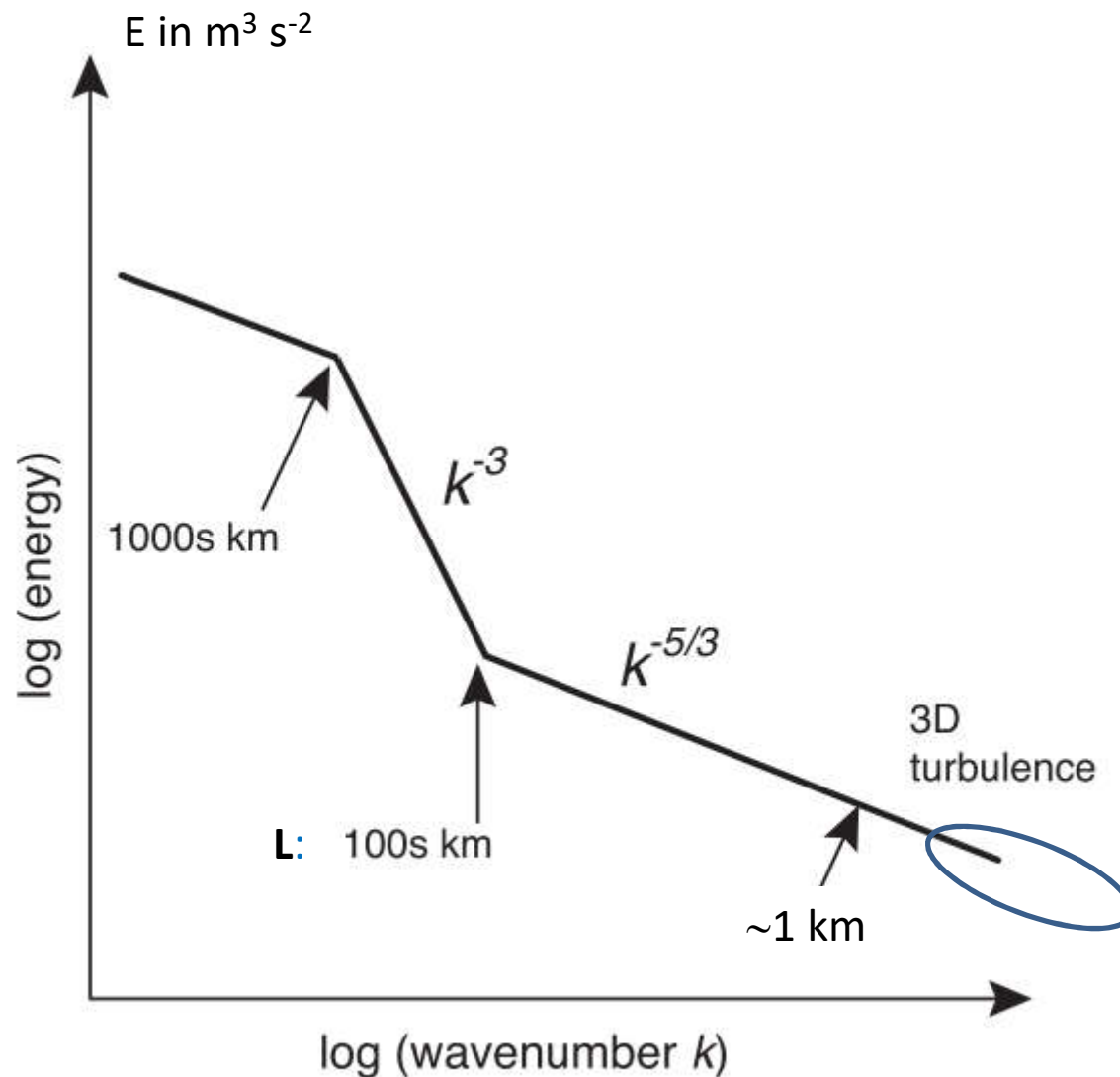


FIG. 1. Schematic of canonical atmospheric kinetic energy spectra.

Small-scale $k^{-5/3}$ spectrum: Inertial-range energy cascade (Kolmogorov, 1941)



Richardson Model

Turbulence scales:

Downscale energy transfer
with energy dissipation
rate ε (unit: $\text{m}^2 \text{s}^{-3}$)

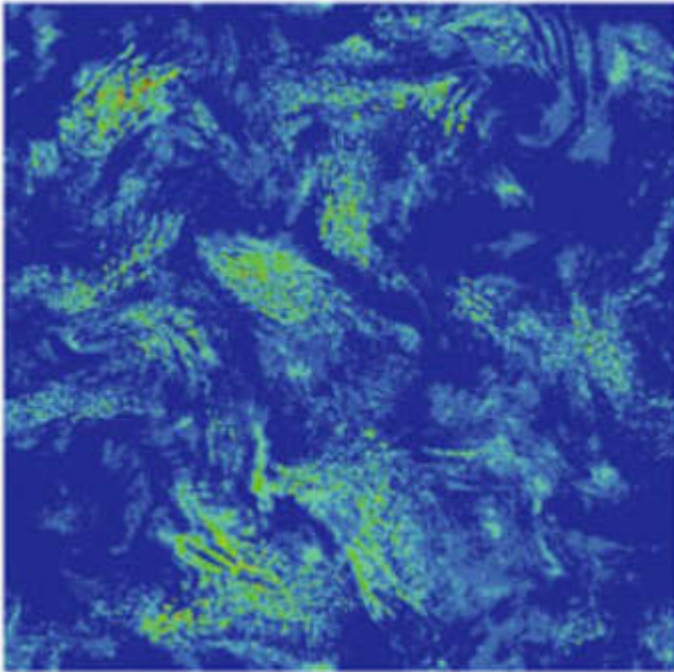
$$E = \varepsilon^{2/3} k^{-5/3}$$

Basic, e.g., for LES SGS

FIG. 1. Schematic of canonical atmospheric kinetic energy spectra.

Stably stratified turbulence

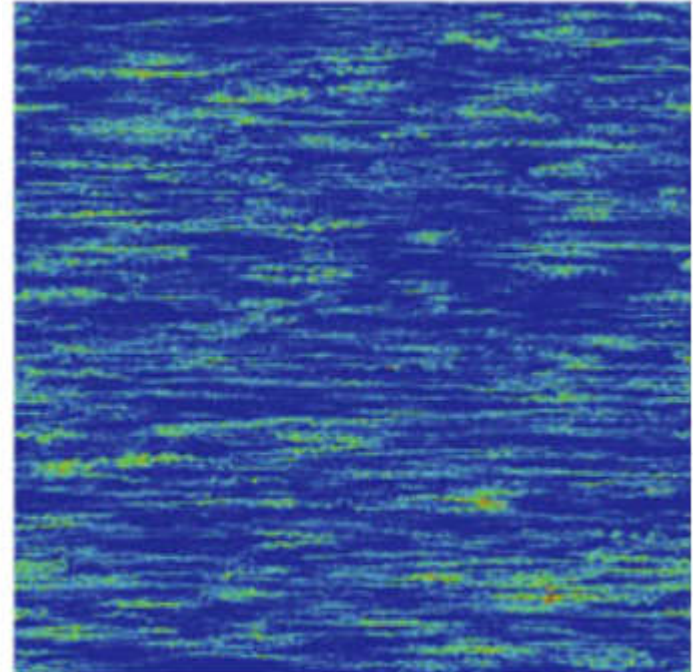
y



x

DNS, 1024^3 grid cells,
homogeneous, stratified turbulence,
forced at large scales
(Kimura and Herring, JFM, 2012)

z



x

Stably stratified turbulence is strongly
anisotropic for scales $>$ Obukhov scale
 $L_o = (\epsilon/N^3)^{1/2}$

Mesoscale $k^{-5/3}$ spectrum: stably stratified turbulence (e.g., Lilly, 1983; Riley and Lindborg, 2008)

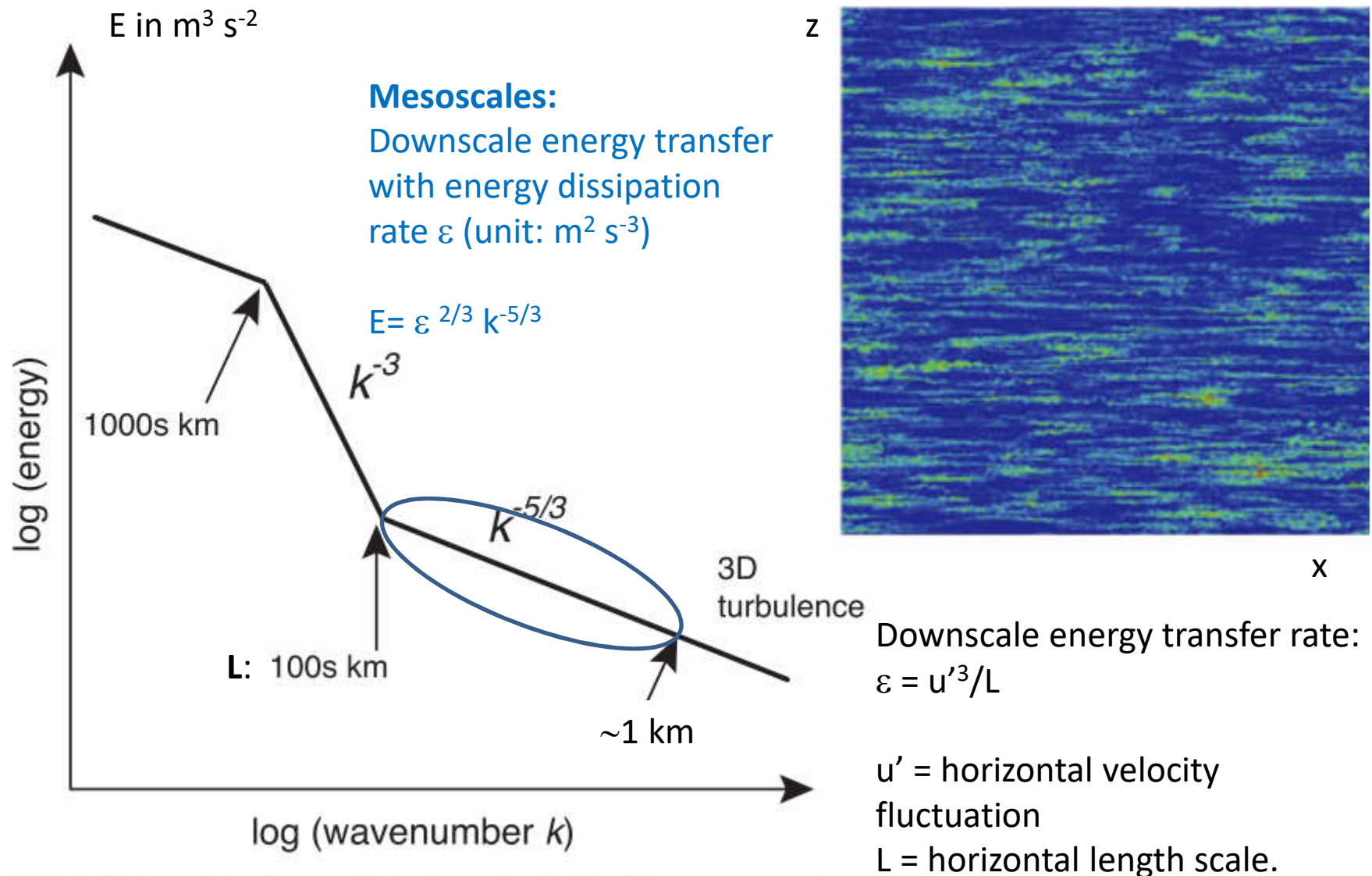
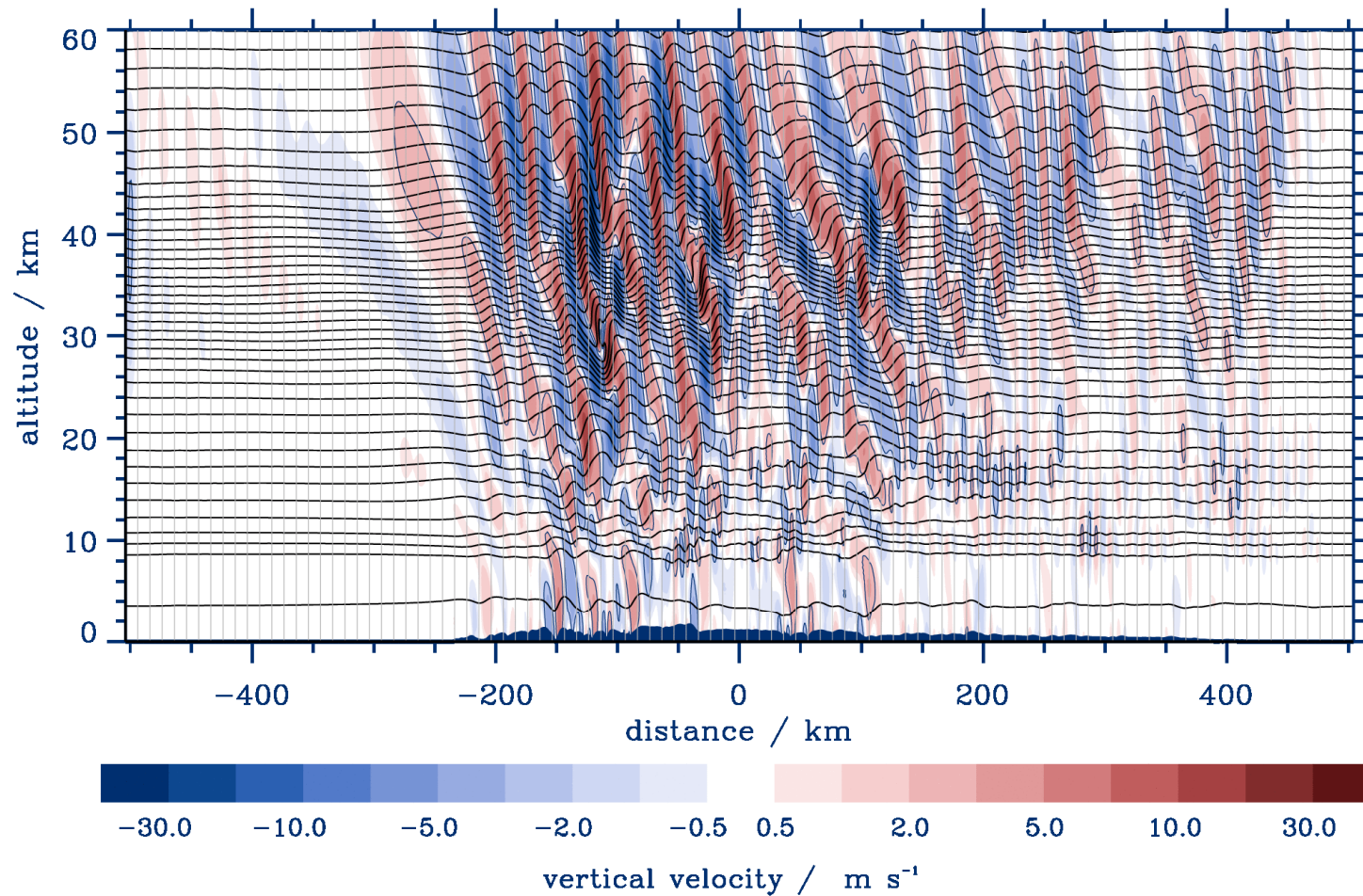


FIG. 1. Schematic of canonical atmospheric kinetic energy spectra.

Gravity waves in stratosphere over mountains

(vertically upward energy transfer, not downscale)



Waves:
disturbances
which travel
over long
distances and
transport energy
and momentum

Dörnbrack (2019).

Helmholtz decomposition (1858) for horizontal velocity

Hermann von Helmholtz (1821-1894)

$$\mathbf{v} = \nabla \times \psi + \nabla \chi$$

(Helmholtz, Crelle J., 1858)

For horizontal velocity $\mathbf{v} = (u, v)$ on a smooth surface with normal \mathbf{k} :

$$\mathbf{v} = \mathbf{k} \times \nabla \psi + \nabla \chi$$

$$\mathbf{v} = \mathbf{v}_R + \mathbf{v}_D, \quad \mathbf{v}_R = \mathbf{k} \times \nabla \psi, \quad \mathbf{v}_D = \nabla \chi. \quad (\text{Wippermann, Beitr. Phys. Atm., 1957})$$

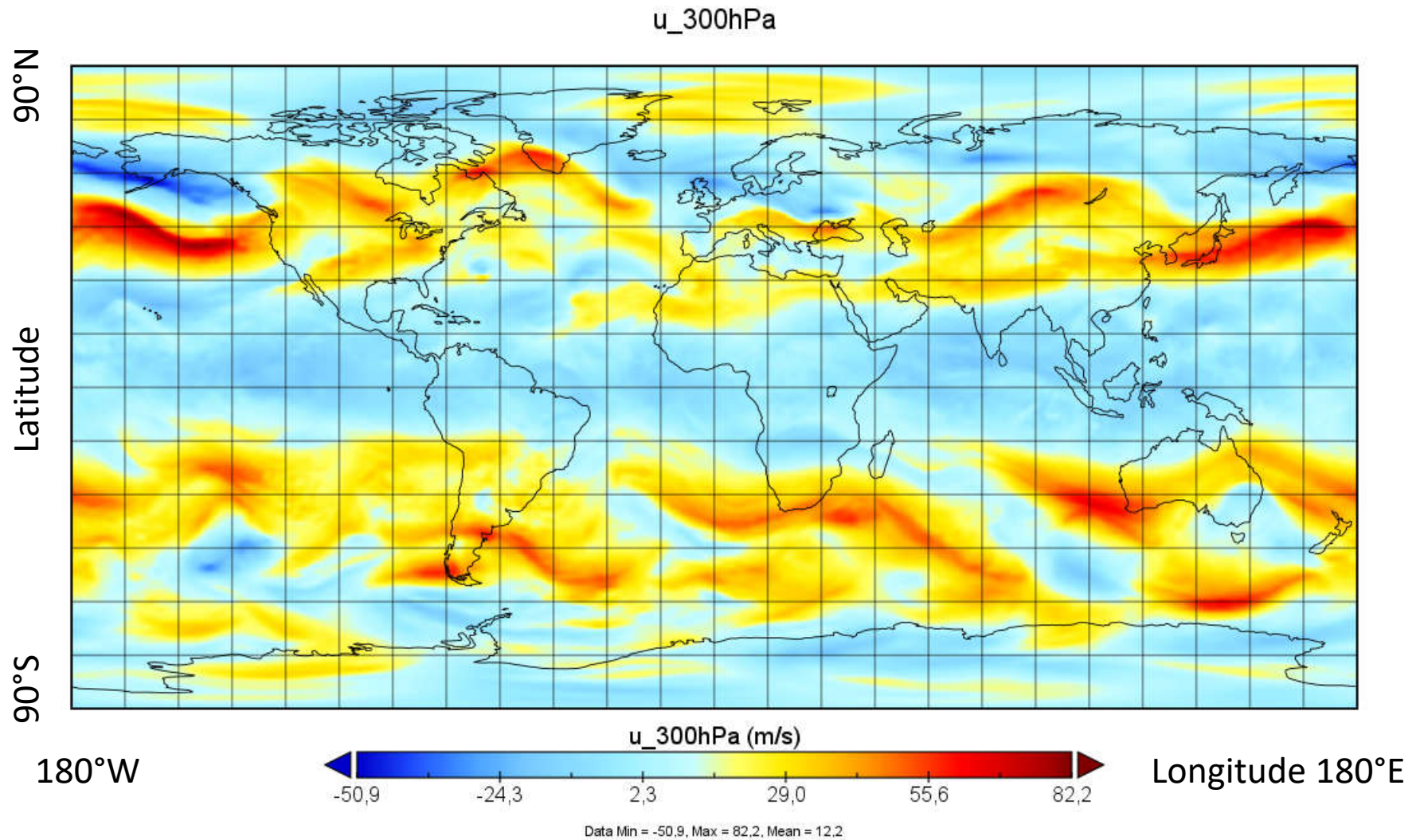
The stream function and velocity potential follow from solutions of Poisson equations

$$\nabla^2 \psi = \zeta = \mathbf{k} \cdot (\nabla \times \mathbf{v})$$

$$\nabla^2 \chi = \delta = \nabla \cdot \mathbf{v}$$

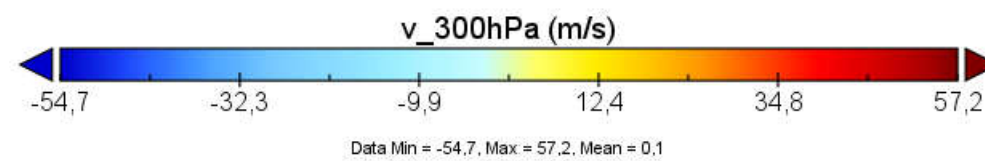
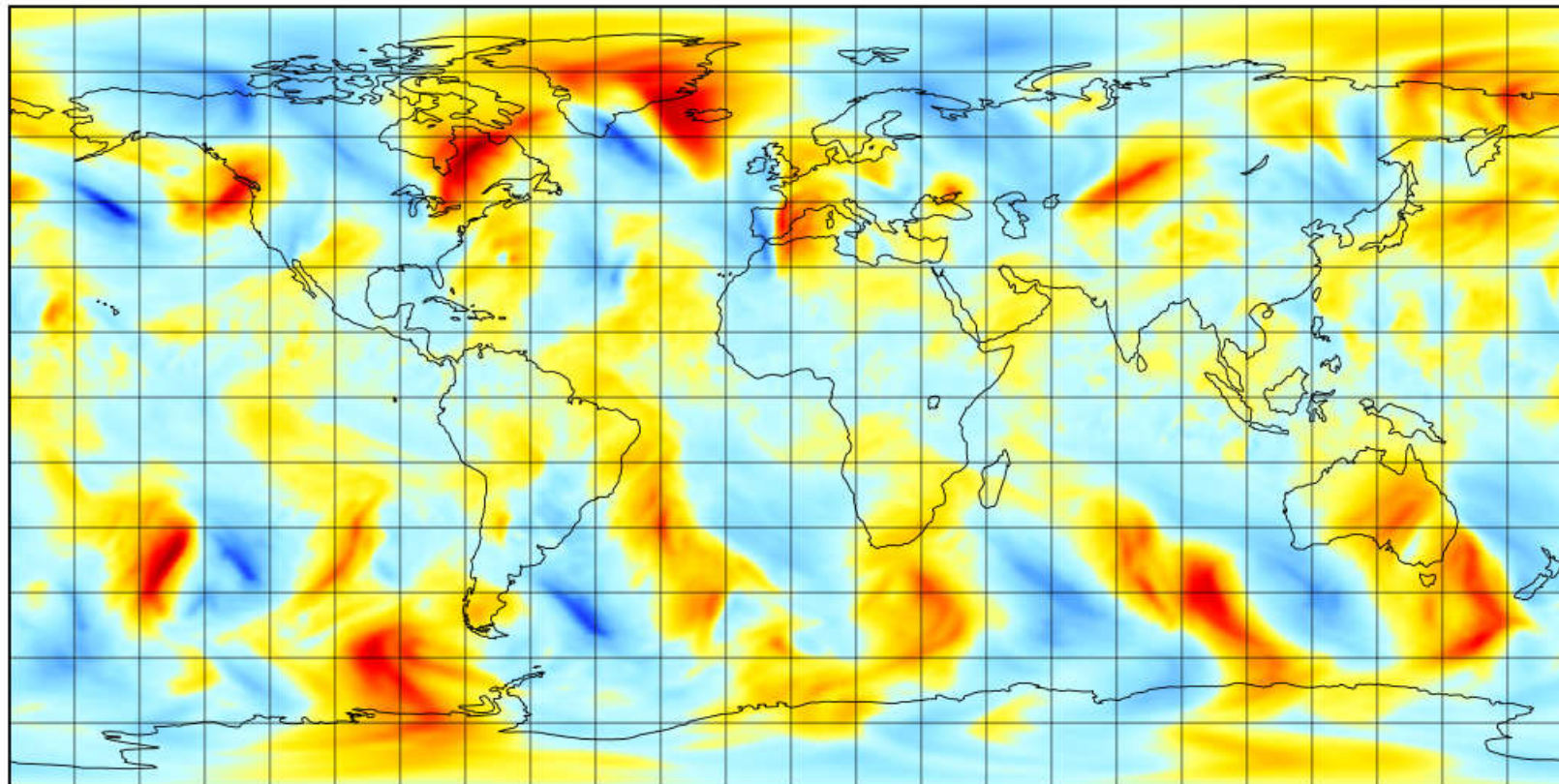
Illustration of Helmholtz decomposition

u, v: horizontal wind components in east and north directions



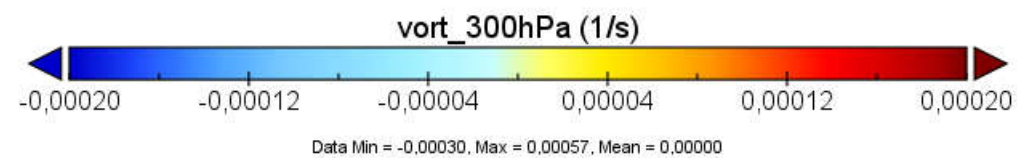
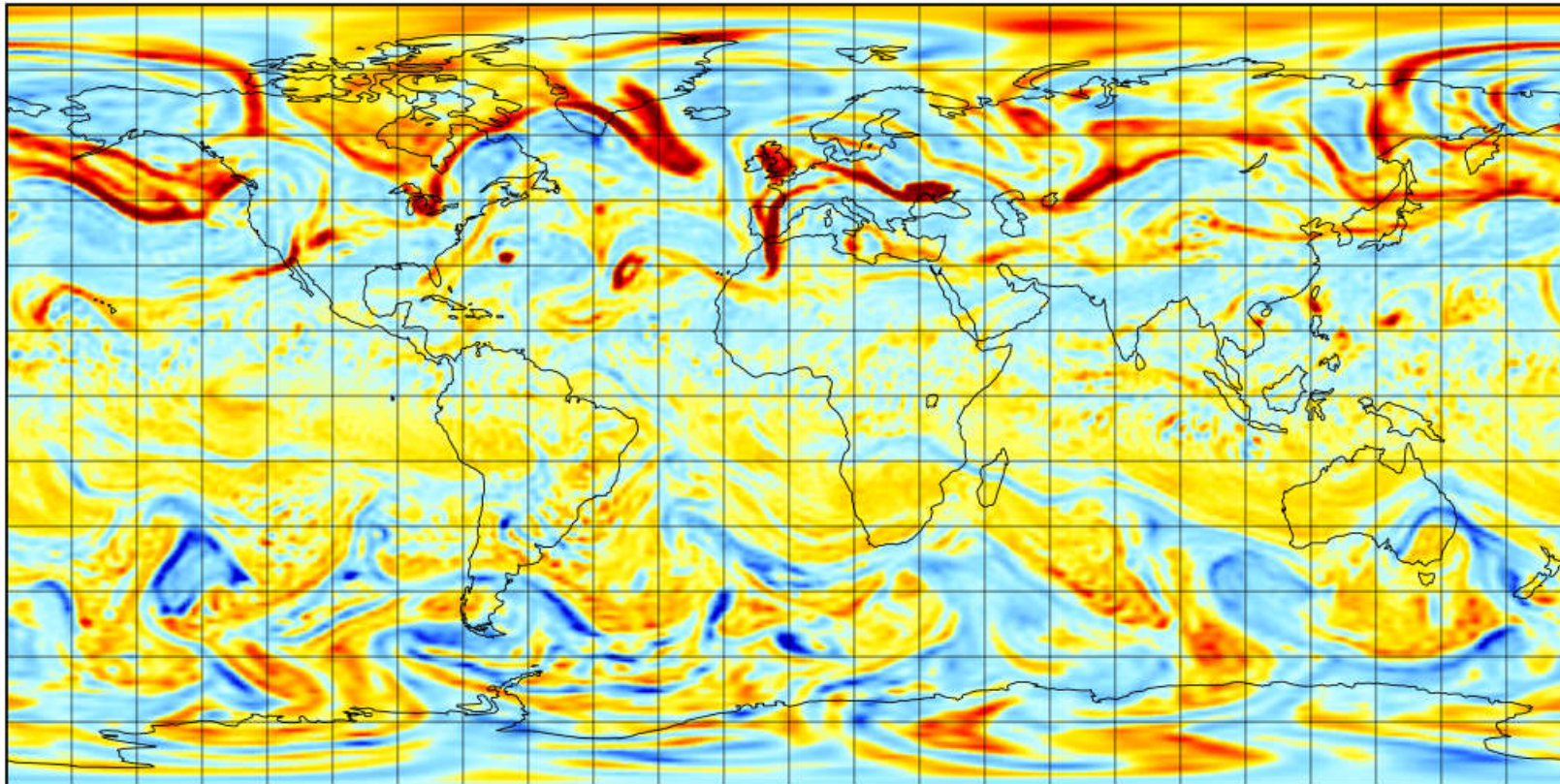
NAWDEX case: 12 UTC 13 Oct 2016, p= 300 hPa \approx 9 km height

v_300hPa



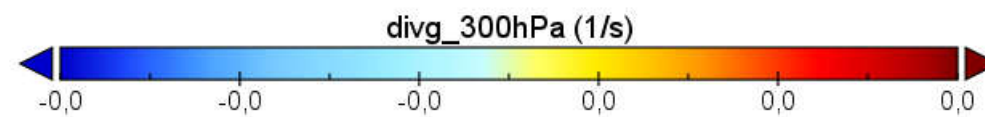
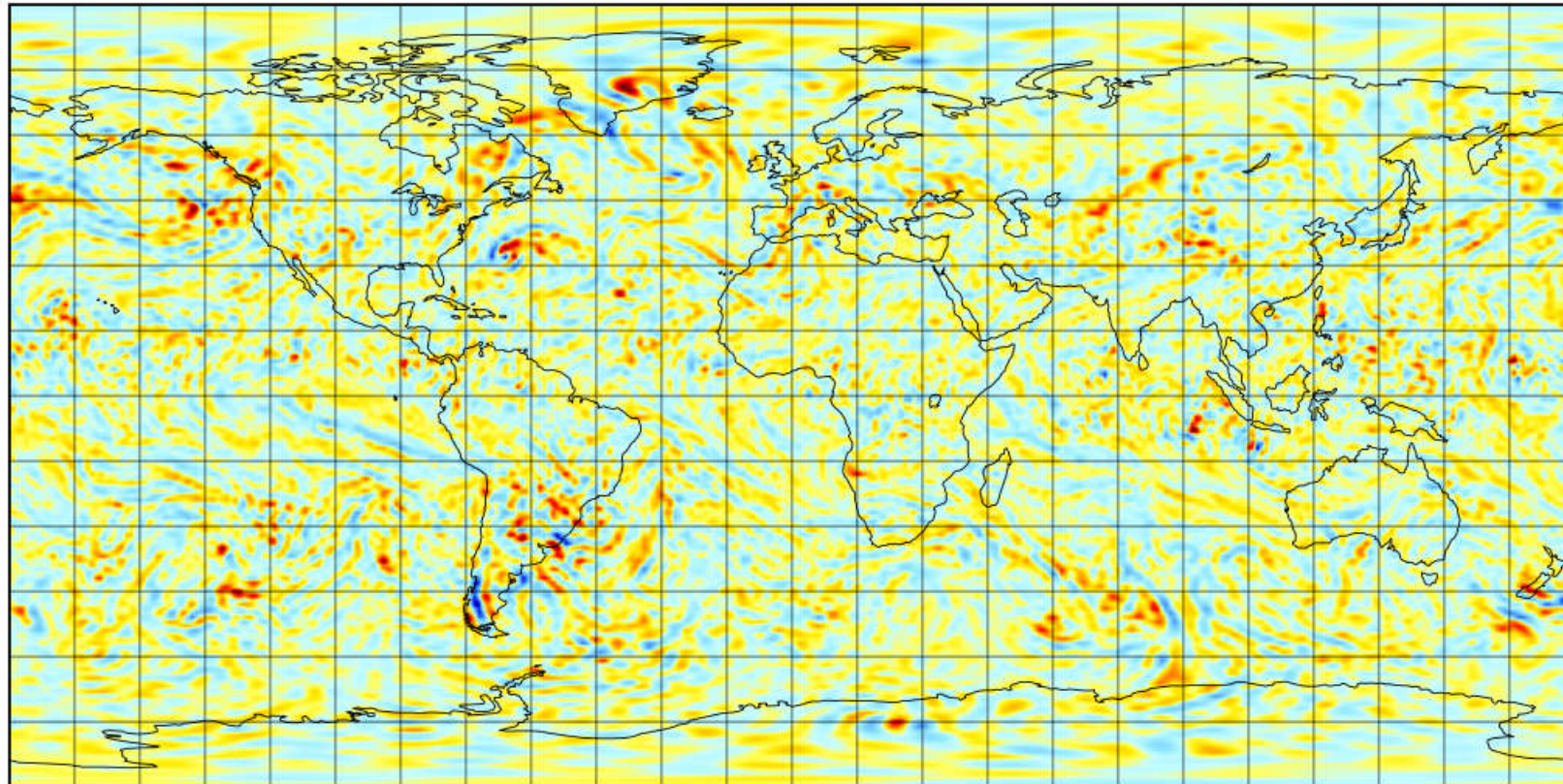
$$\zeta = \mathbf{k} \cdot (\nabla \times \mathbf{v})$$

vort_300hPa



$$\delta = \nabla \cdot \mathbf{v}$$

divg_300hPa

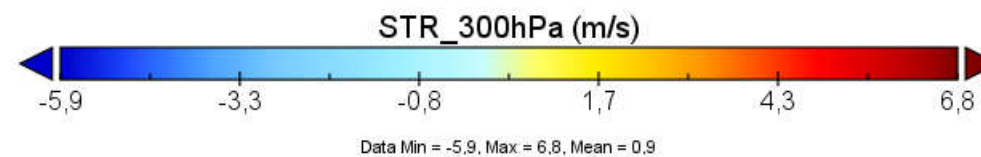
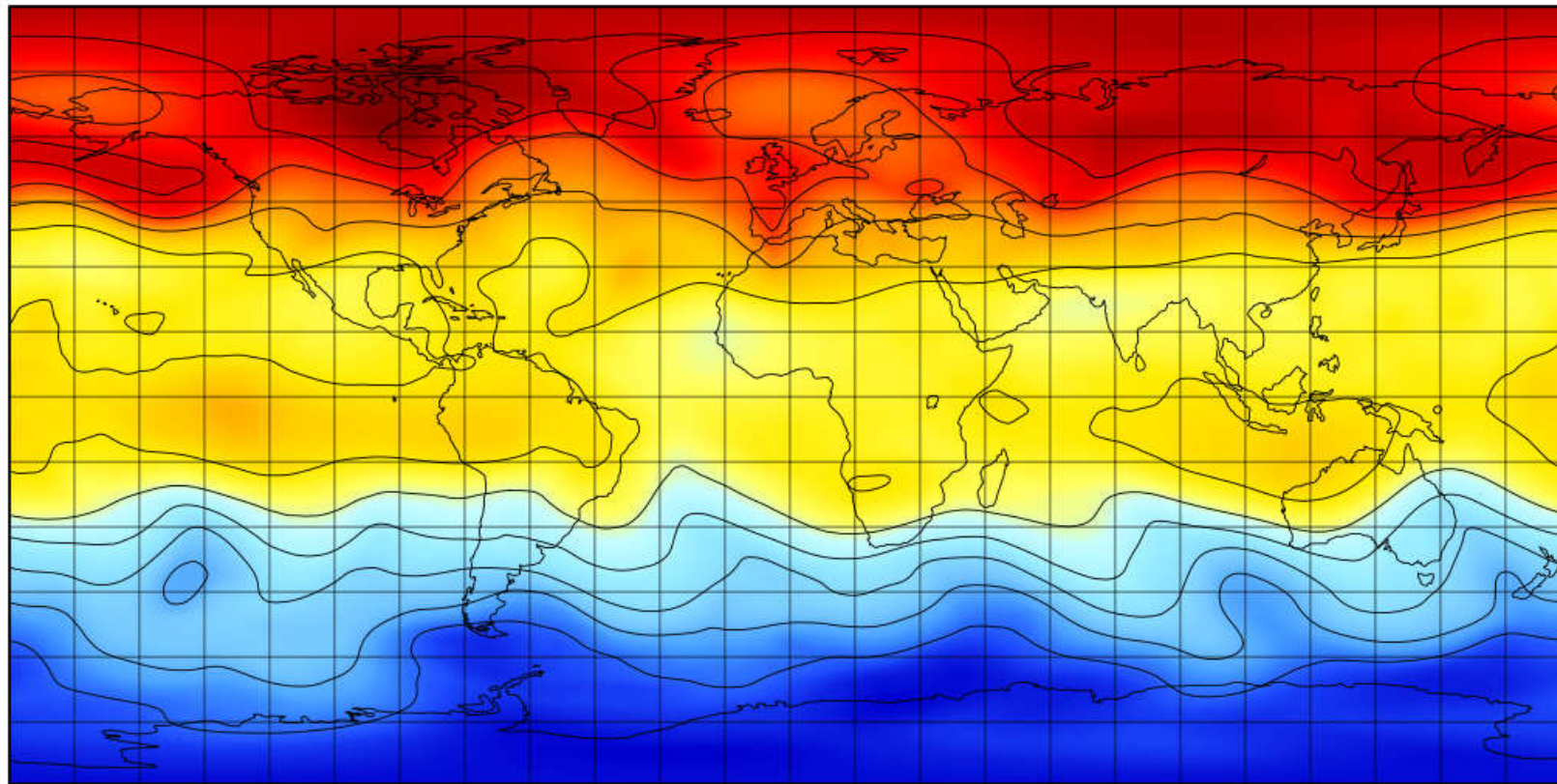


Data Min = -0.0, Max = 0.0, Mean = -0.0

$$\zeta = \mathbf{k} \cdot (\nabla \times \mathbf{v}) = \frac{1}{R \cos \theta} \left[\frac{\partial v}{\partial \lambda} - \frac{\partial u \cos \varphi}{\partial \varphi} \right] = \nabla^2 \psi$$

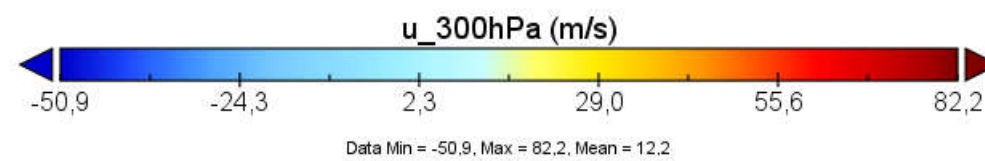
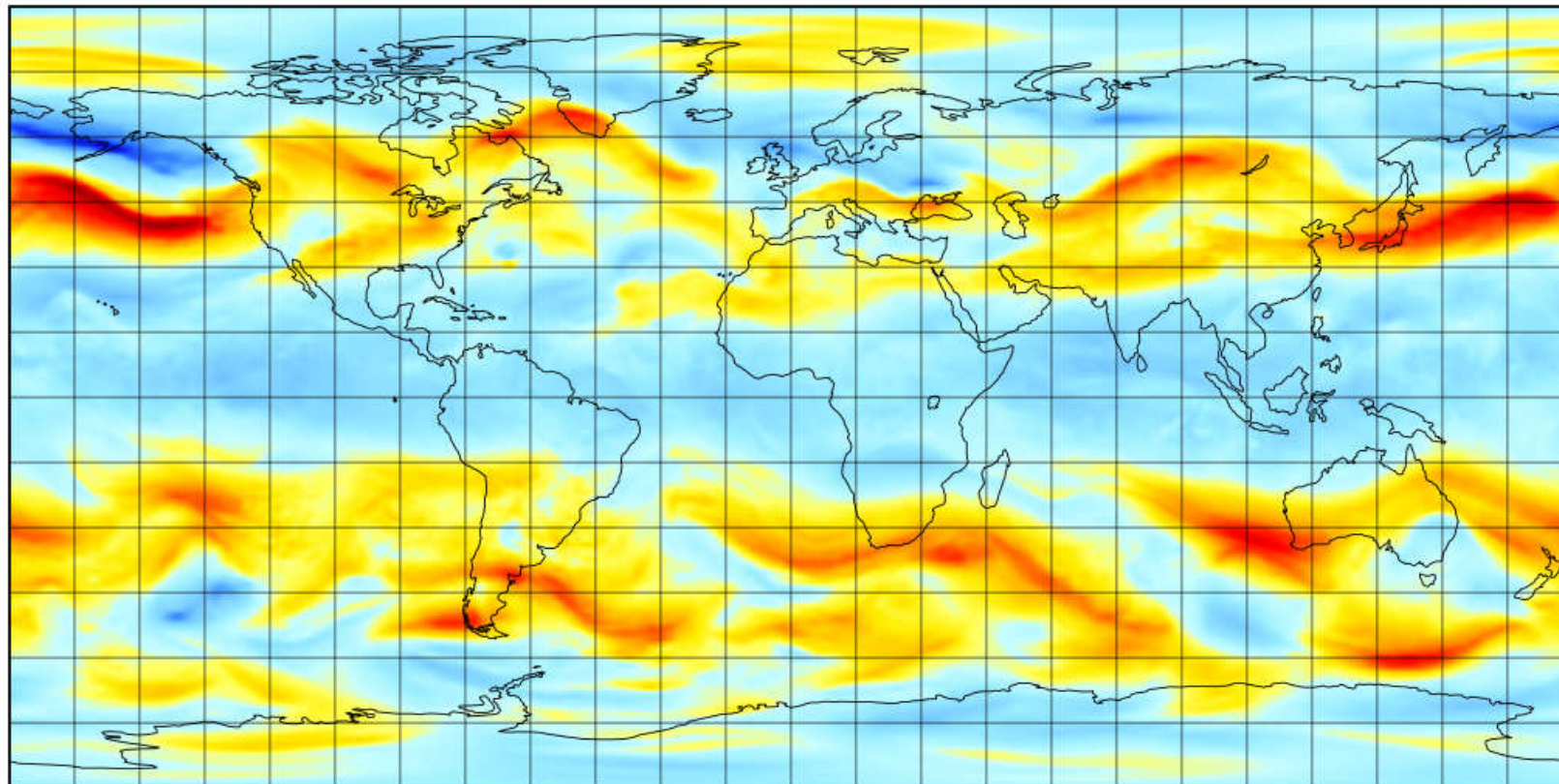
$$\text{STR} = \psi / (\pi R)$$

STR_300hPa



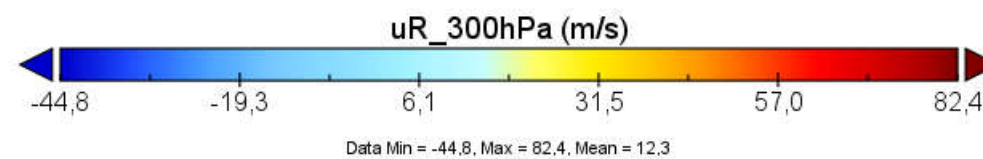
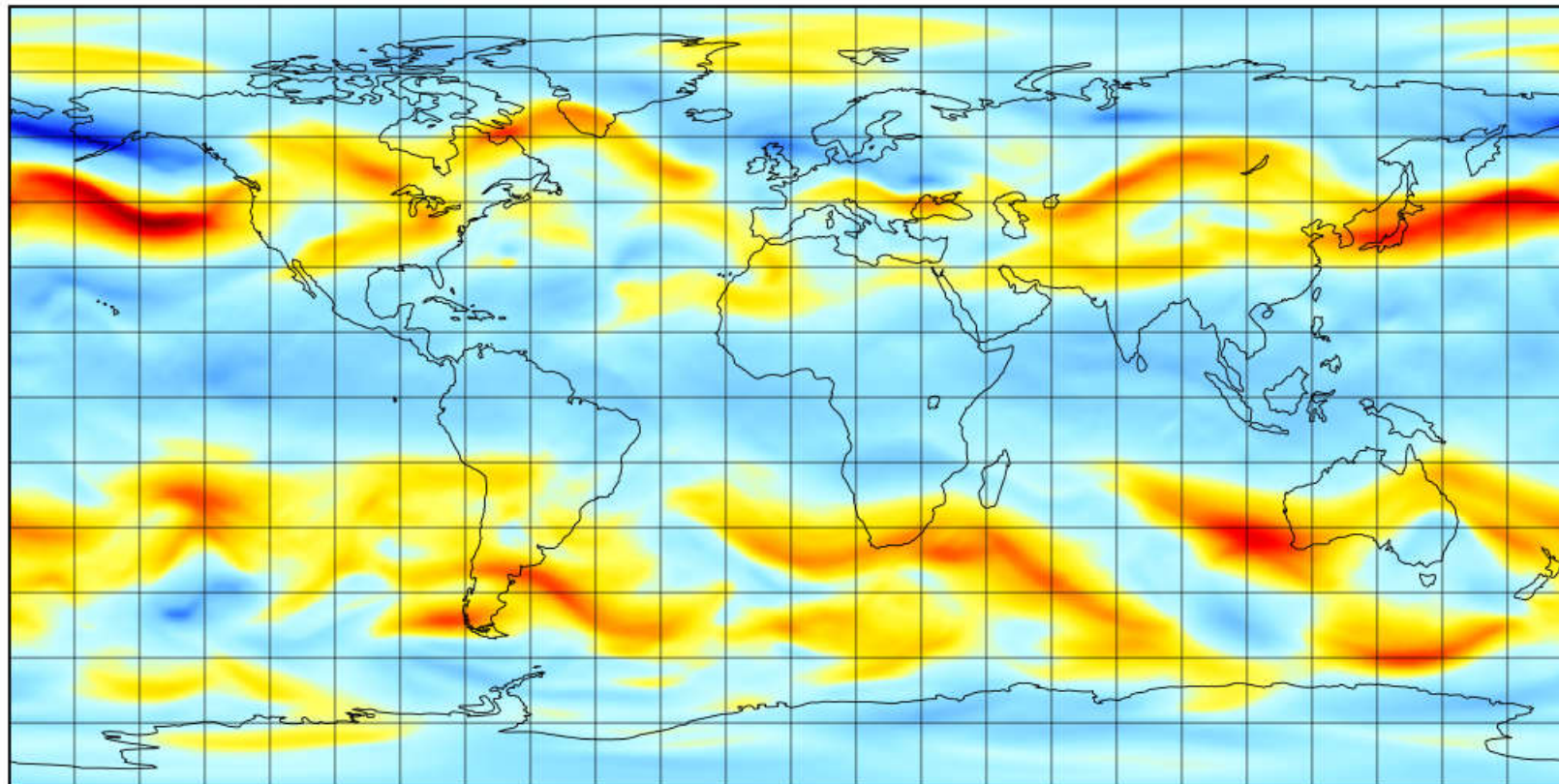
Solution of Helmholtz equation after spherical harmonics decomposition (Swarztrauber et al. 1993) using SPHEREPACK (2011)

u_300hPa



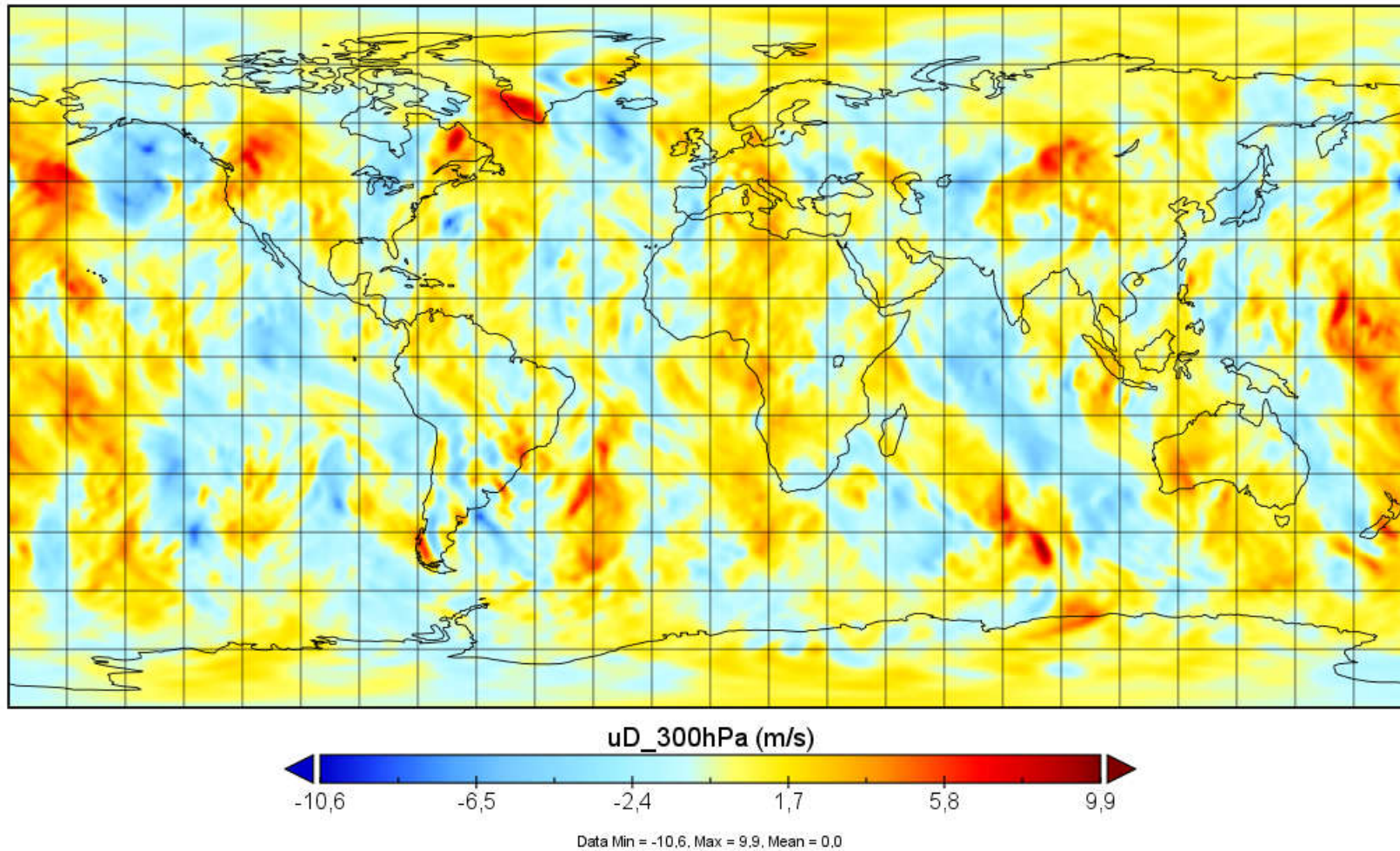
$$u_R = -\frac{1}{R} \frac{\partial \psi}{\partial \phi},$$

uR_300hPa

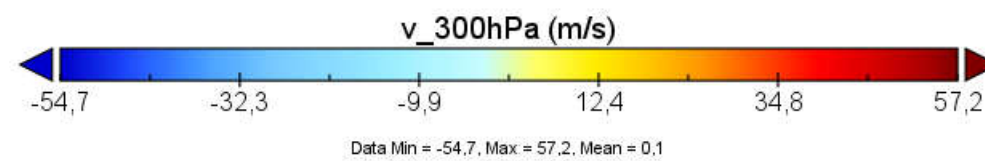
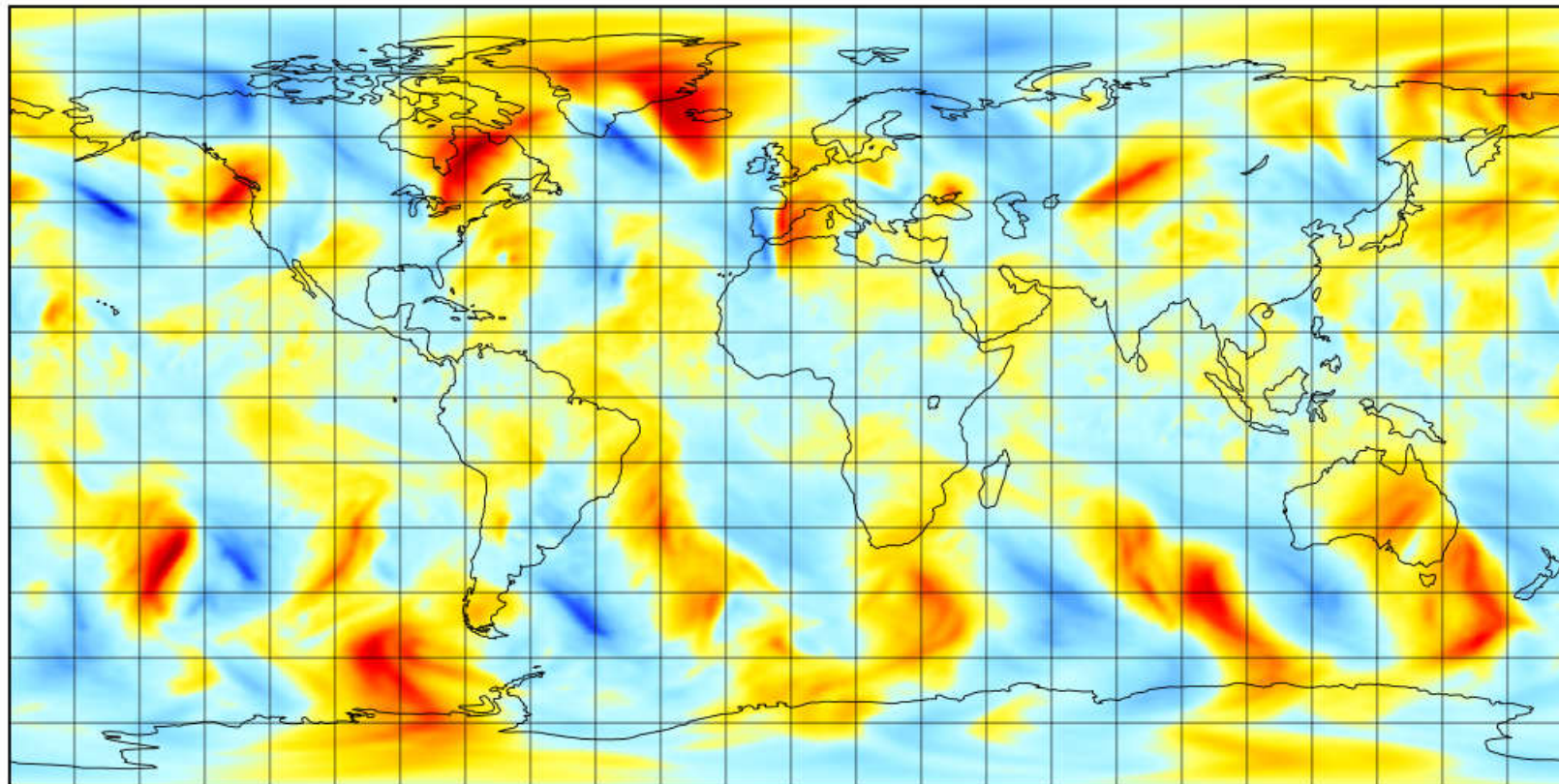


$$u_D = \frac{1}{R \cos \varphi} \frac{\partial \chi}{\partial \lambda}$$

uD_300hPa

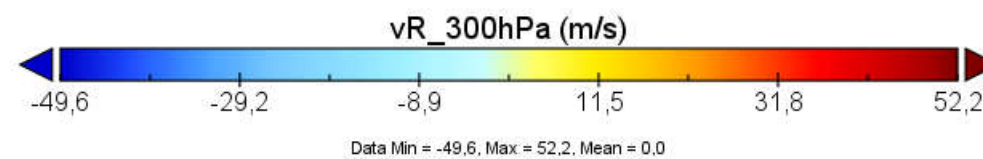
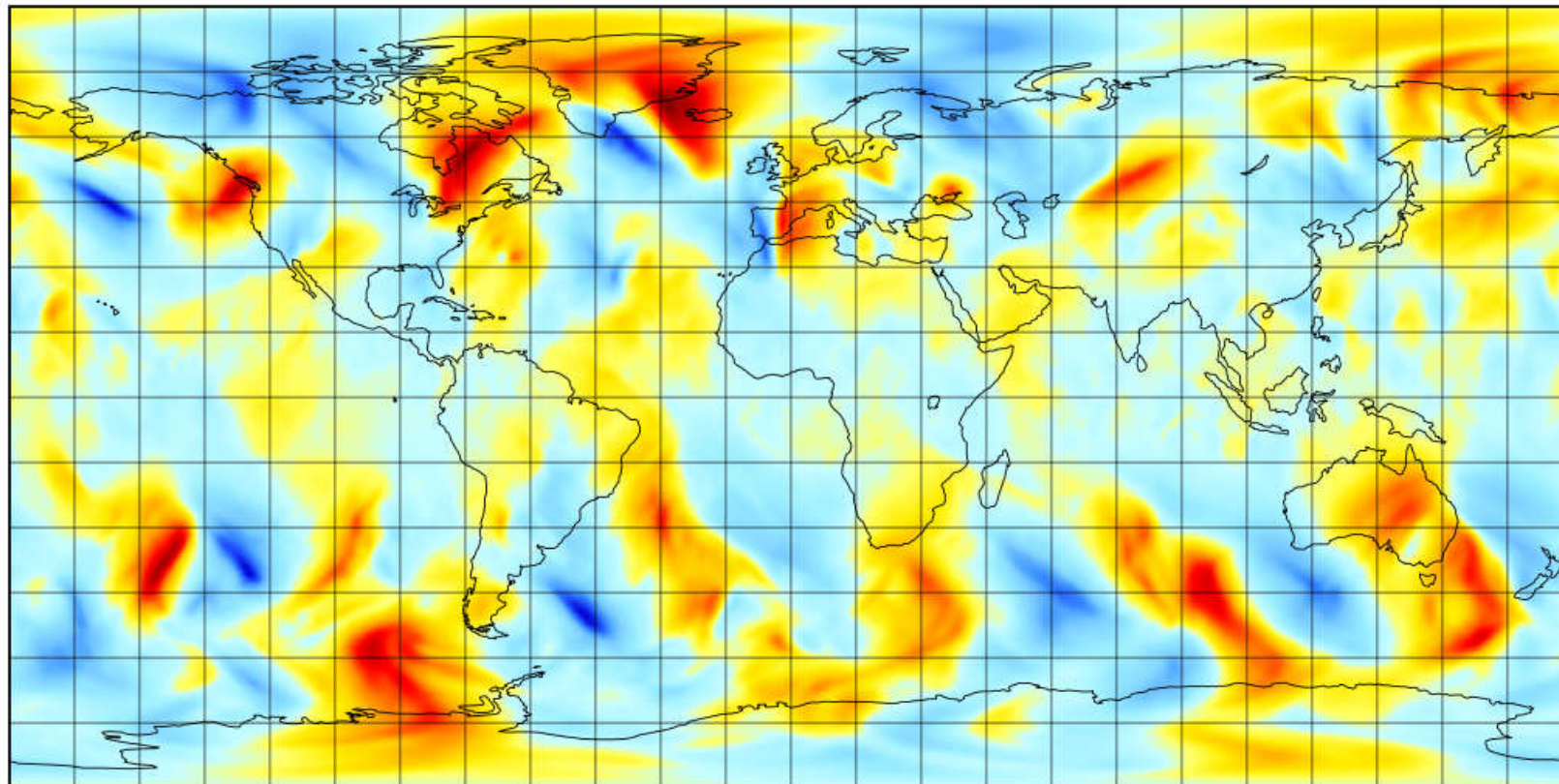


v_300hPa



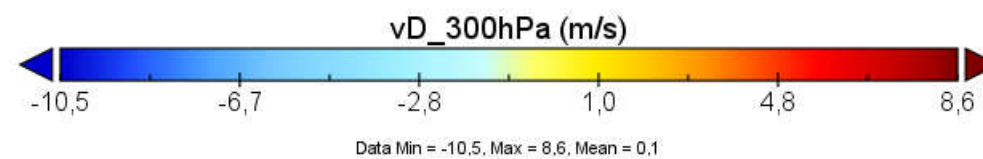
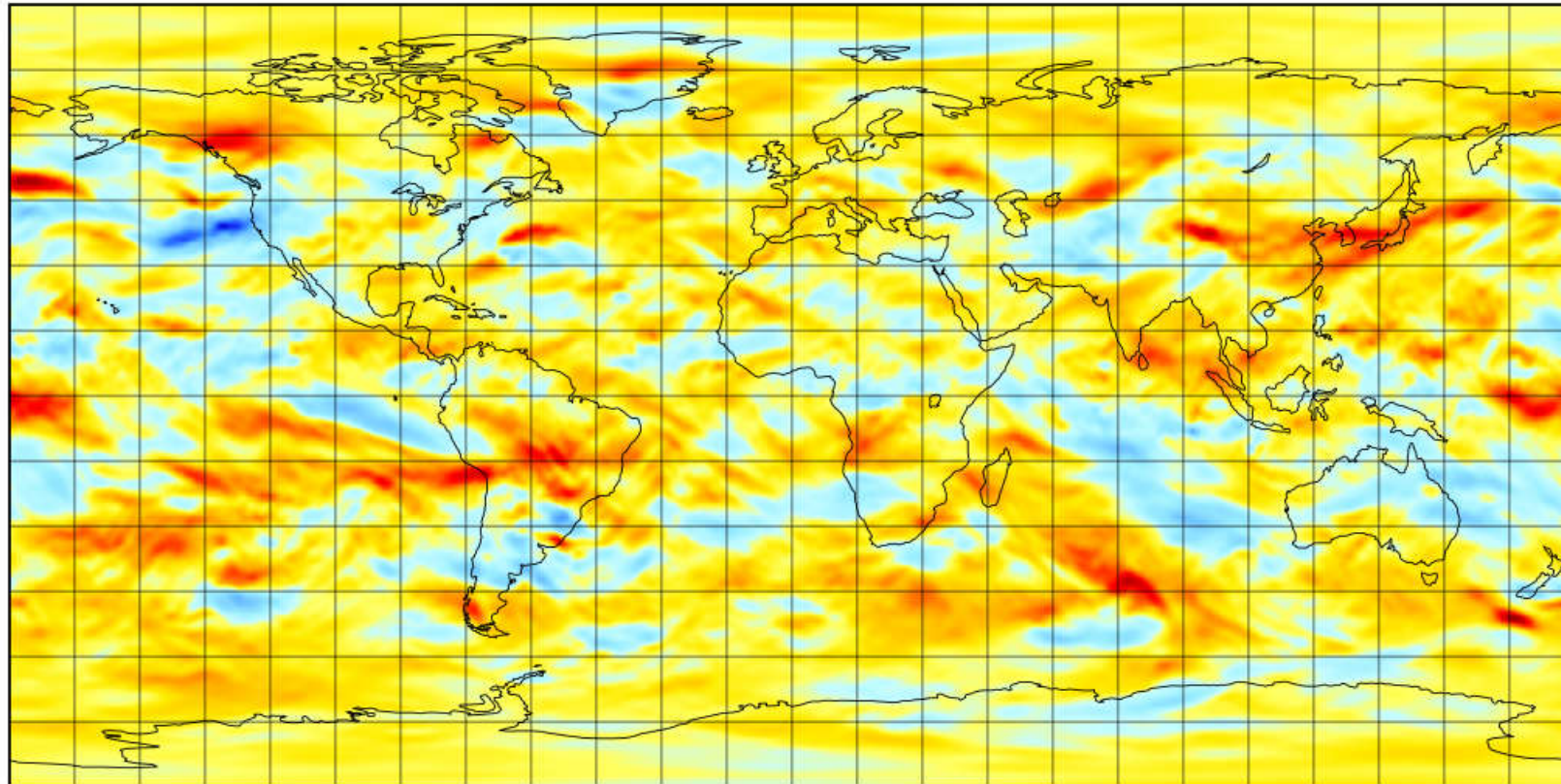
$$v_R = \frac{1}{R \cos \varphi} \frac{\partial \psi}{\partial \lambda}$$

vR_300hPa



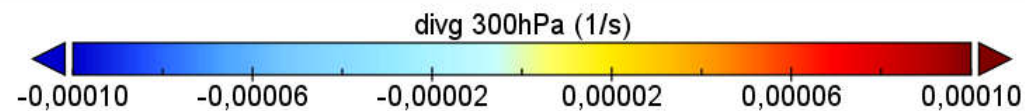
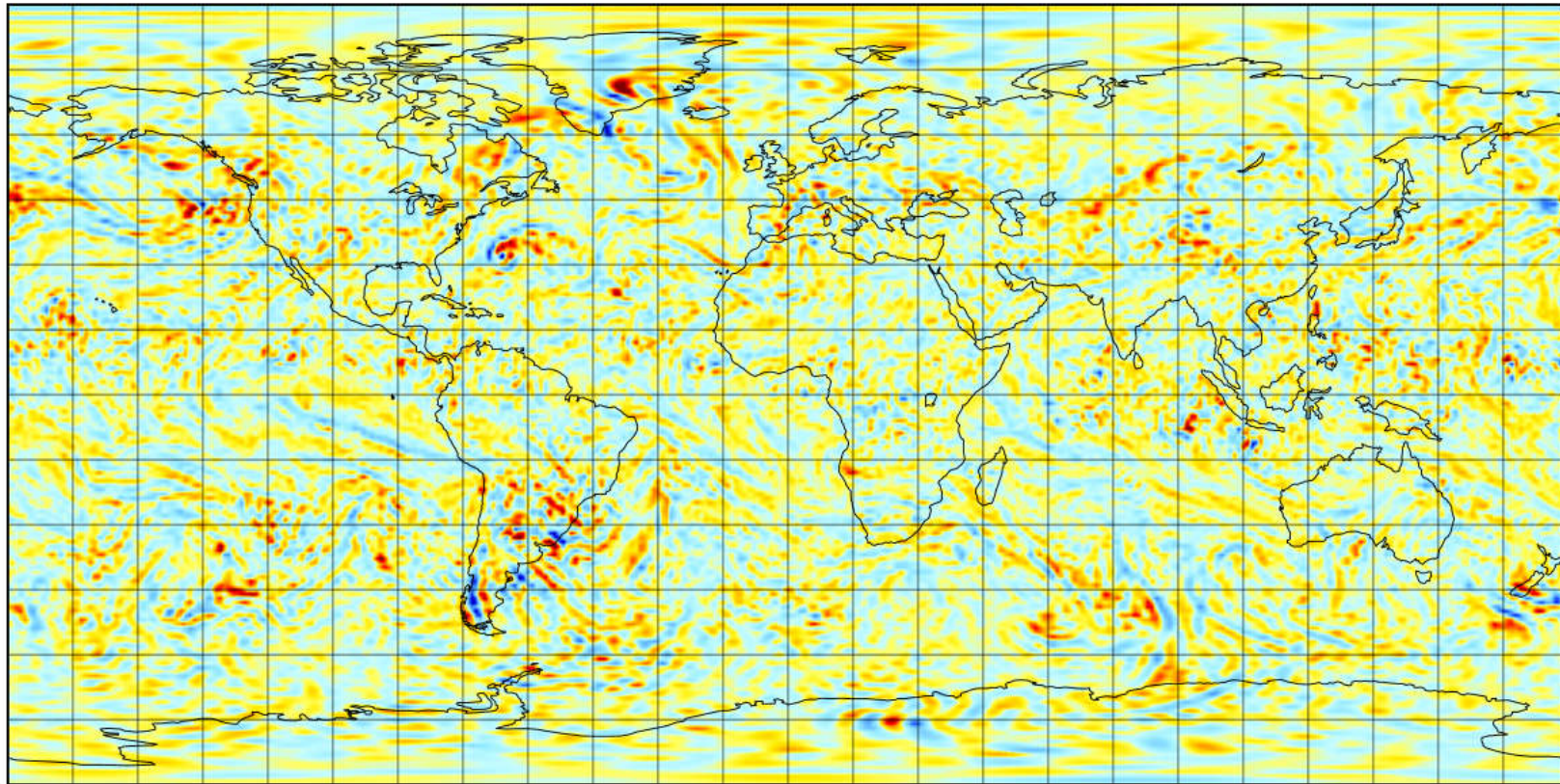
$$v_D = \frac{1}{R} \frac{\partial \chi}{\partial \varphi}$$

vD_300hPa



$$\delta = \nabla \cdot \mathbf{v} = \frac{1}{R \cos \varphi} \frac{\partial u}{\partial \lambda} + \frac{1}{R \cos \varphi} \frac{\partial (v \cos \varphi)}{\partial \varphi} = \nabla^2 \chi$$

divg 300hPa

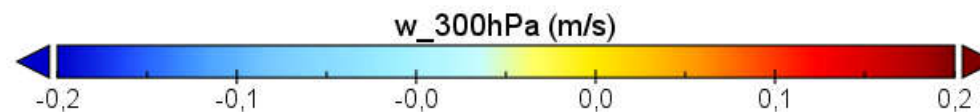
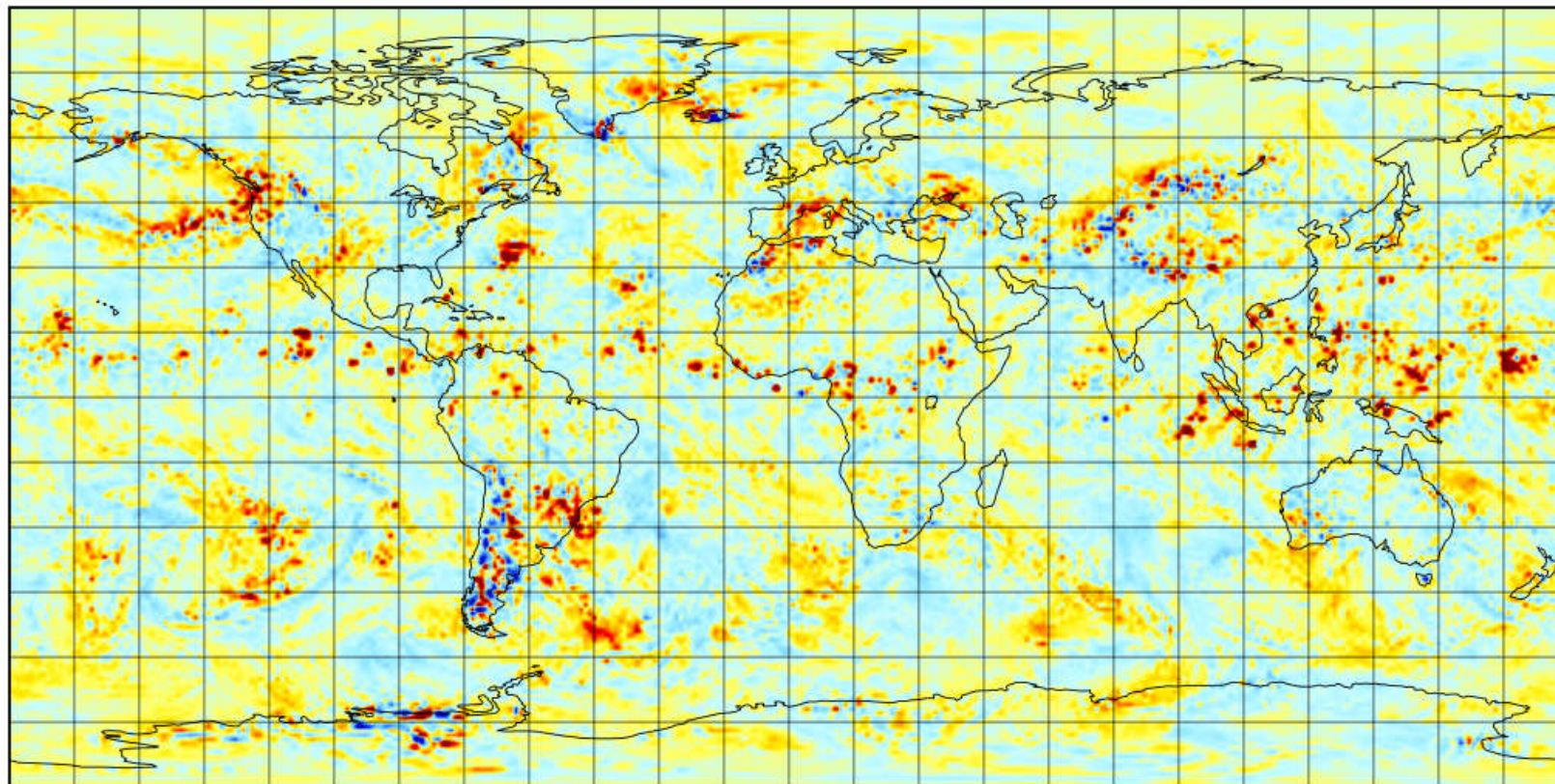


Data Min = -0,00018, Max = 0,00015, Mean = 0,00000

$$\frac{\partial w}{\partial z} = - \left(\frac{\partial u_D}{\partial x} + \frac{\partial v_D}{\partial y} \right) = -\delta, \quad w(z) - w(0) = - \int_0^z \delta \, dz$$

Note: only the divergent velocity components determine vertical wind

w_300hPa



Data Min = -0.7, Max = 2.4, Mean = 0.0

Exchange between potential and horizontal kinetic energy Catalyzed by divergent horizontal velocity (w)

$$\mathbf{v} = \mathbf{k} \times \nabla\psi + \nabla\chi$$

work of divergent motions against gradients of geopotential

potential +
internal
energy

rotational
energy

divergent
energy

The diagram illustrates the exchange between three energy components: potential + internal energy, rotational energy, and divergent energy. The equations are arranged vertically, with arrows indicating the flow of energy between them.

$$\begin{aligned} \frac{\partial}{\partial t} (\bar{\bar{P}} + \bar{\bar{I}}) &= + \overline{\nabla\chi \nabla\Phi} + \bar{\bar{dQ}} \\ \frac{\partial}{\partial t} \frac{\overline{(\nabla\psi)^2}}{2} &= - \overline{(f + \nabla^2\psi) \nabla\chi \nabla\psi} - \overline{\nabla^2\chi \frac{(\nabla\psi)^2}{2}} - \overline{\omega \mathbf{k} \left[\nabla\psi \times \nabla \frac{\partial\chi}{\partial\psi} \right]} \\ \frac{\partial}{\partial t} \frac{\overline{(\nabla\chi)^2}}{2} &= - \overline{\nabla\chi \nabla\Phi} + \overline{(f + \nabla^2\psi) \nabla\chi \nabla\psi} + \overline{\nabla^2\chi \frac{(\nabla\psi)^2}{2}} + \overline{\omega \mathbf{k} \left[\nabla\psi \times \nabla \frac{\partial\chi}{\partial p} \right]} \end{aligned}$$

Arrows indicate the following exchanges:

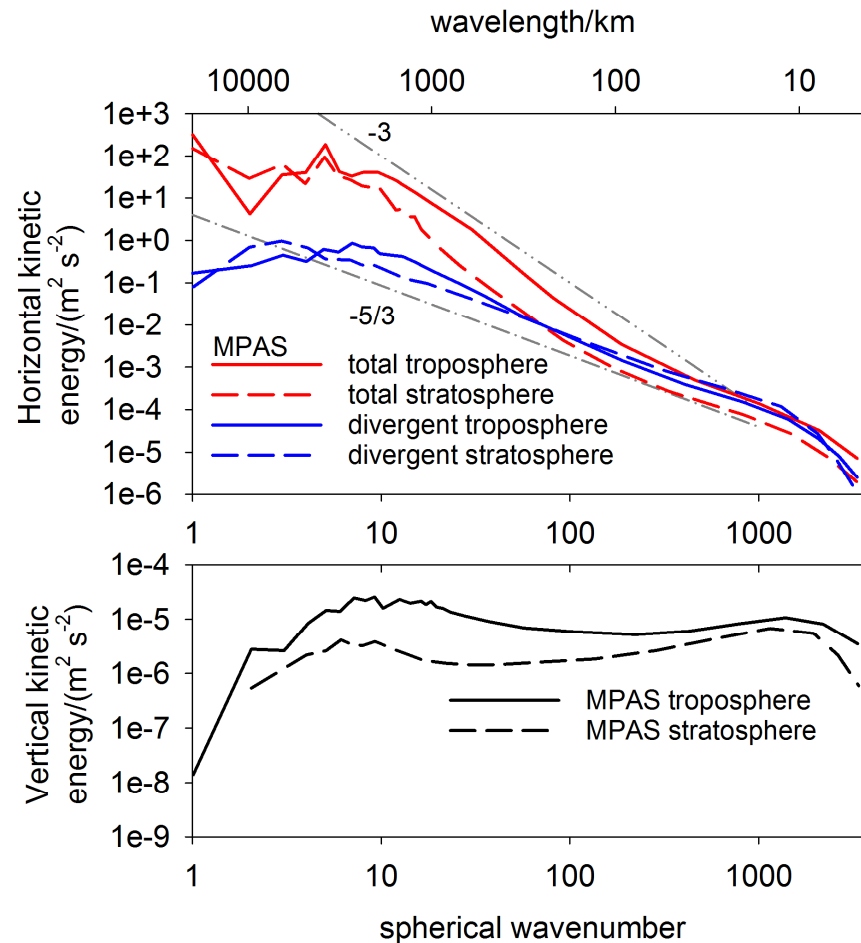
- A vertical double-headed arrow connects the first and second equations.
- A vertical double-headed arrow connects the second and third equations.
- A vertical double-headed arrow connects the first and third equations.

(Wippermann, 1957;
see also Lorenz 1960; Wiin-Nielsen, 1968; Chen and Wiin-Nielsen, 1976)

What do we know about horizontal w spectra

from simulations
from aircraft measurements?

Global numerical simulation spectra



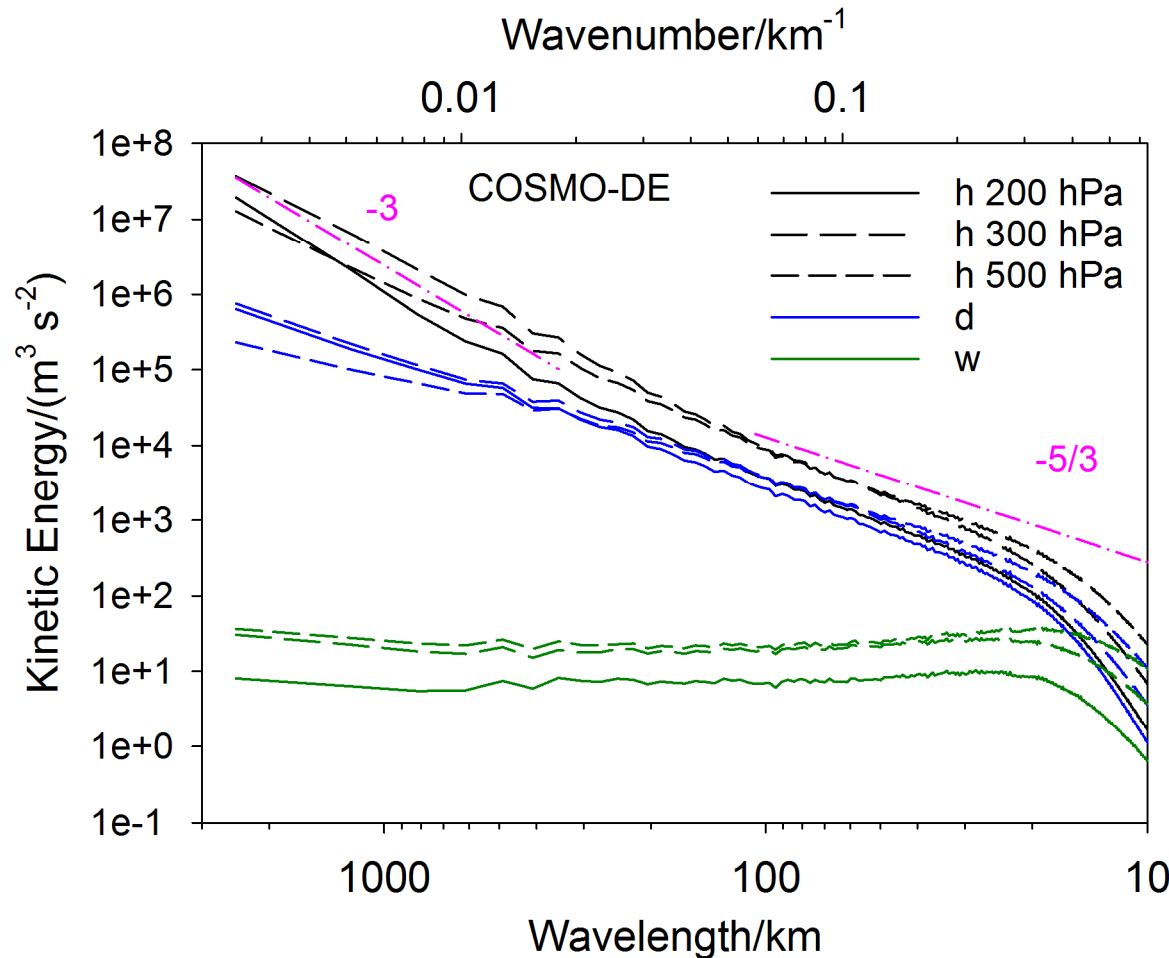
-3 and -5/3-spectrum as
in canonical spectrum

near -2 and -5/3
divergent spectrum,
 $d = E_d / (E_d + E_r) \approx 0.5$
at mesoscales

different w-spectra in
TRO and STR
with unexplained
maxima

(Skamarock et al., 2014)

COSMO-DE: 3 years of regional numerical weather prediction data



Data courtesy Tobias Selz

spectrum only slightly different from canonical spectrum

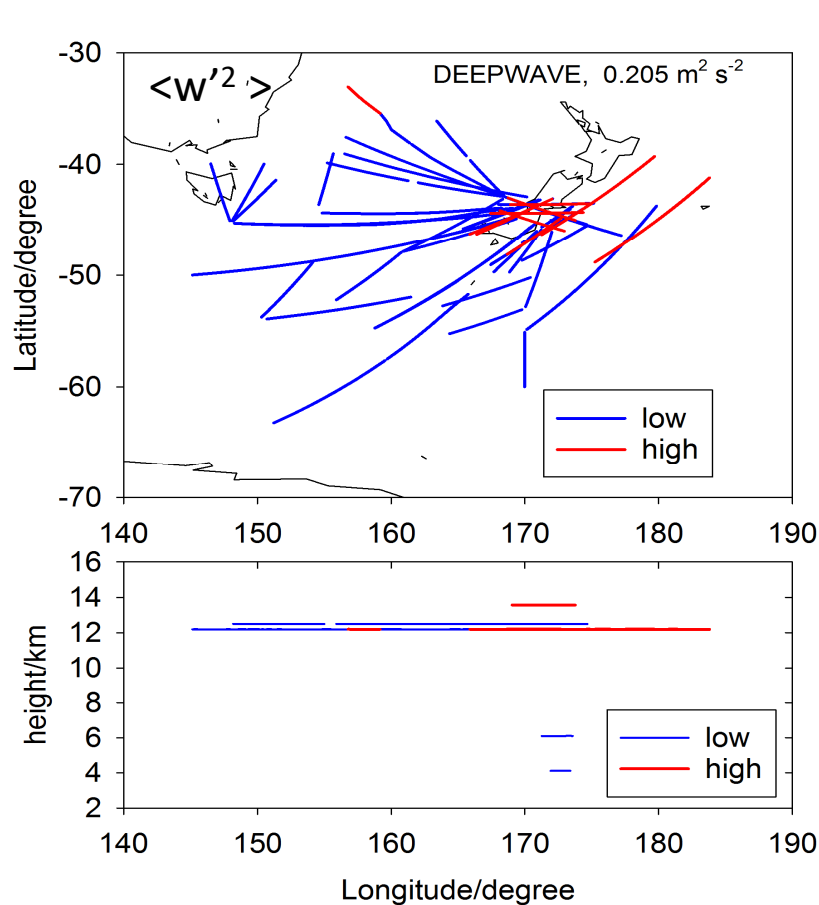
-2 and -5/3
divergent spectrum,
 $d \approx 0.5$ at mesoscales

flat w-spectrum
with maximum possibly due to convection

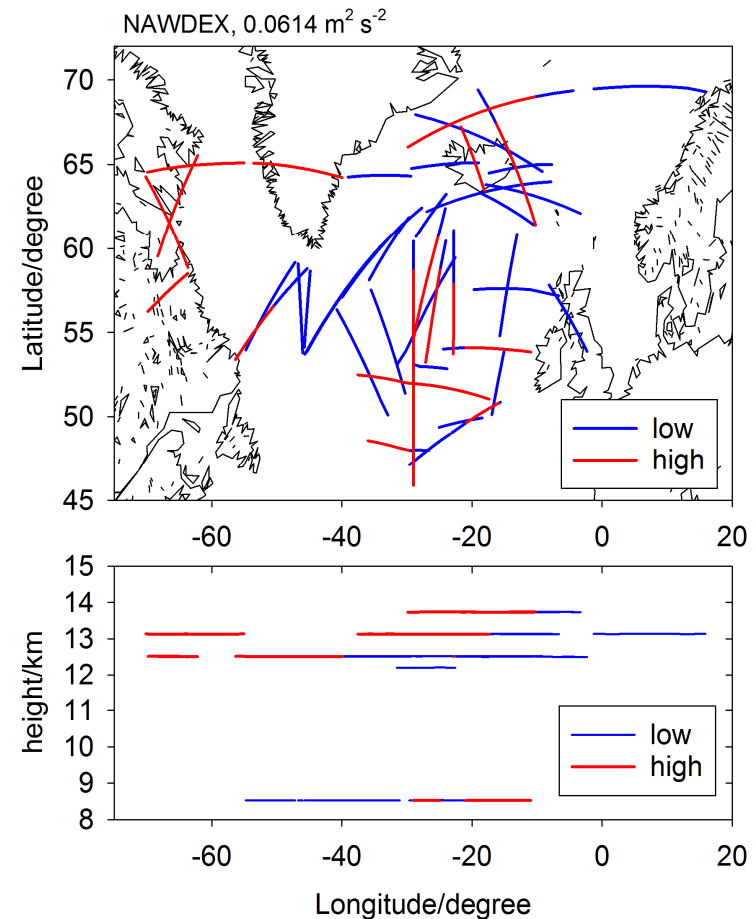
(Selz, Bierdel, Craig, JAS, 2019)

DEEPWAVE (D, 2014) and NAWDEX (N, 2016)

airborne measurements in the upper troposphere/lower stratosphere (UTLS), 180 and 107 legs, 2048 s each



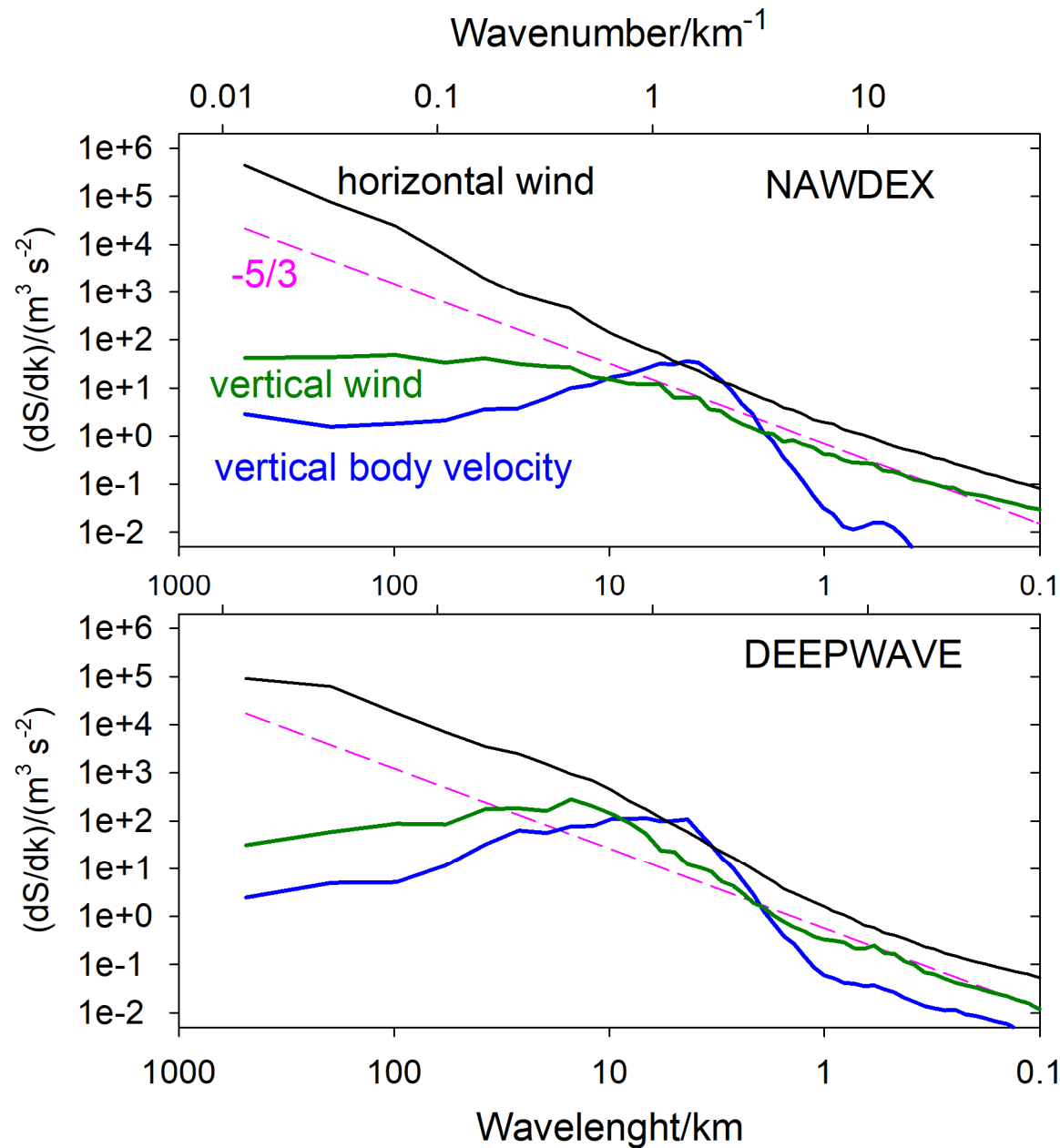
Fritts et al. (2016),
NSF-GV (HIAPER) NCAR EOL



Schäfler et al. (2018),
HALO DLR-FX



Measured velocity spectra, mean over all legs



How to explain the **w** spectra?

Impact of vertical body motions on **w** measurement?

Hypothesis:

The spectrum of vertical velocities E_w ,
as a function of wavenumber k and height h ,
is related to the spectrum of horizontal velocities E_h

- 1) at large scales: to E_d by continuity,
- 2) at small scales: to E_h by dynamics towards local isotropy

$$E_w(k, h) = \frac{\alpha(h_{\text{eff}} k)^2}{\alpha + (h_{\text{eff}} k)^2} d E_h(k, h), \quad h_{\text{eff}} = \beta h$$

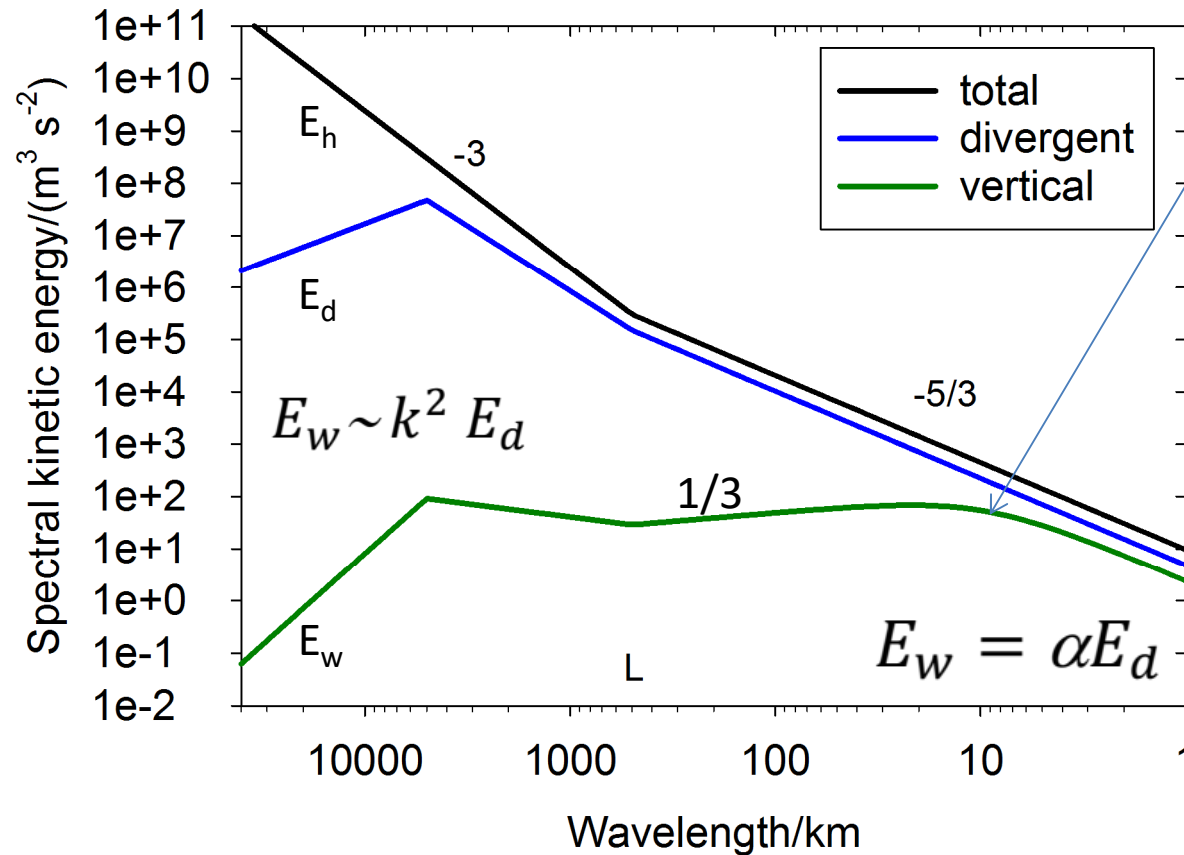
$\alpha \approx 0.5$ for stratified turbulence

$\beta \approx 0.1$ to 0.5 , depending on vertical variability of horizontal motions

$d \approx 0.5$, divergent energy fraction at mesoscales

For formal derivation, see J. Atmos Sci (2019)

A schematic sketch of E_w



A mesoscale maximum in the w-spectrum occurs if the divergent horizontal velocity spectrum E_d has a slope flatter than -2

$$E_w(k, h) = \frac{\alpha(h_{\text{eff}} k)^2}{\alpha + (h_{\text{eff}} k)^2} E_d(k, h), \quad h_{\text{eff}} = \beta h$$

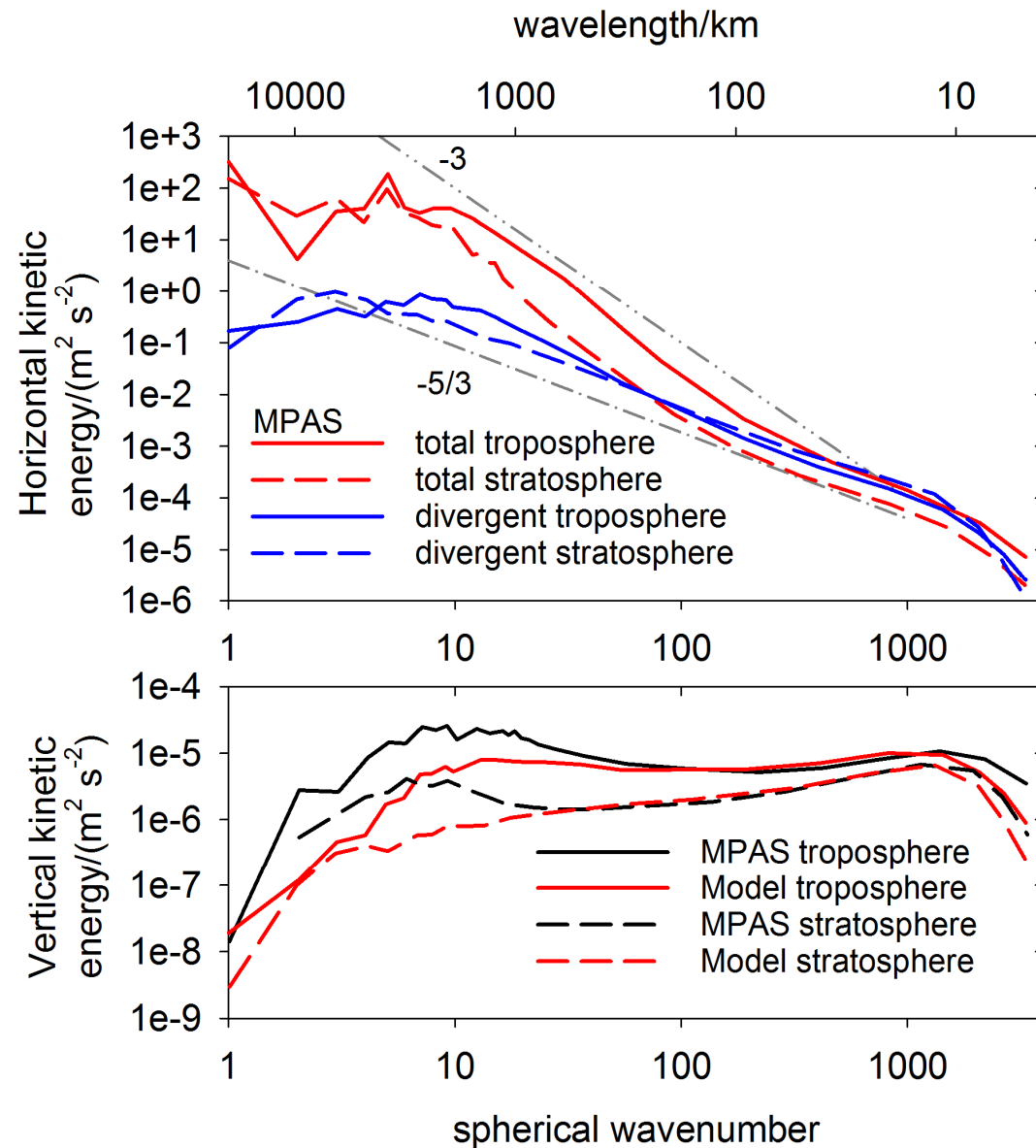
$$h=10 \text{ km}, \alpha=1/2, \beta=0.11, d=1/2$$

Comparison of the model spectrum with

global simulations

aircraft measurements

Comparison of the **w-model** to the global simulation w-spectra

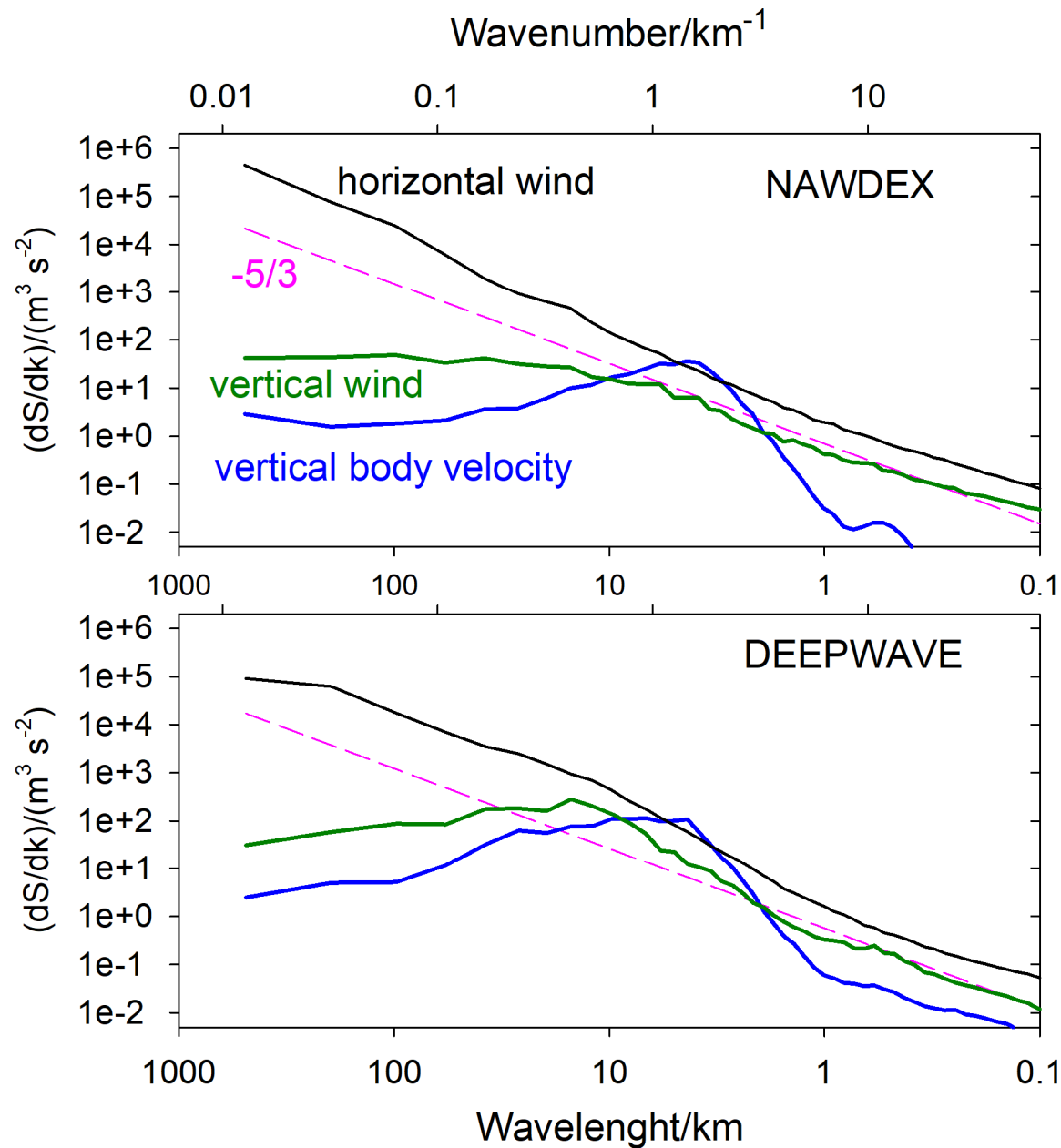


The proposed model is consistent with the MPAS results.

Some deviations were to be expected because of

- non-2d-isotropy
- surface orography

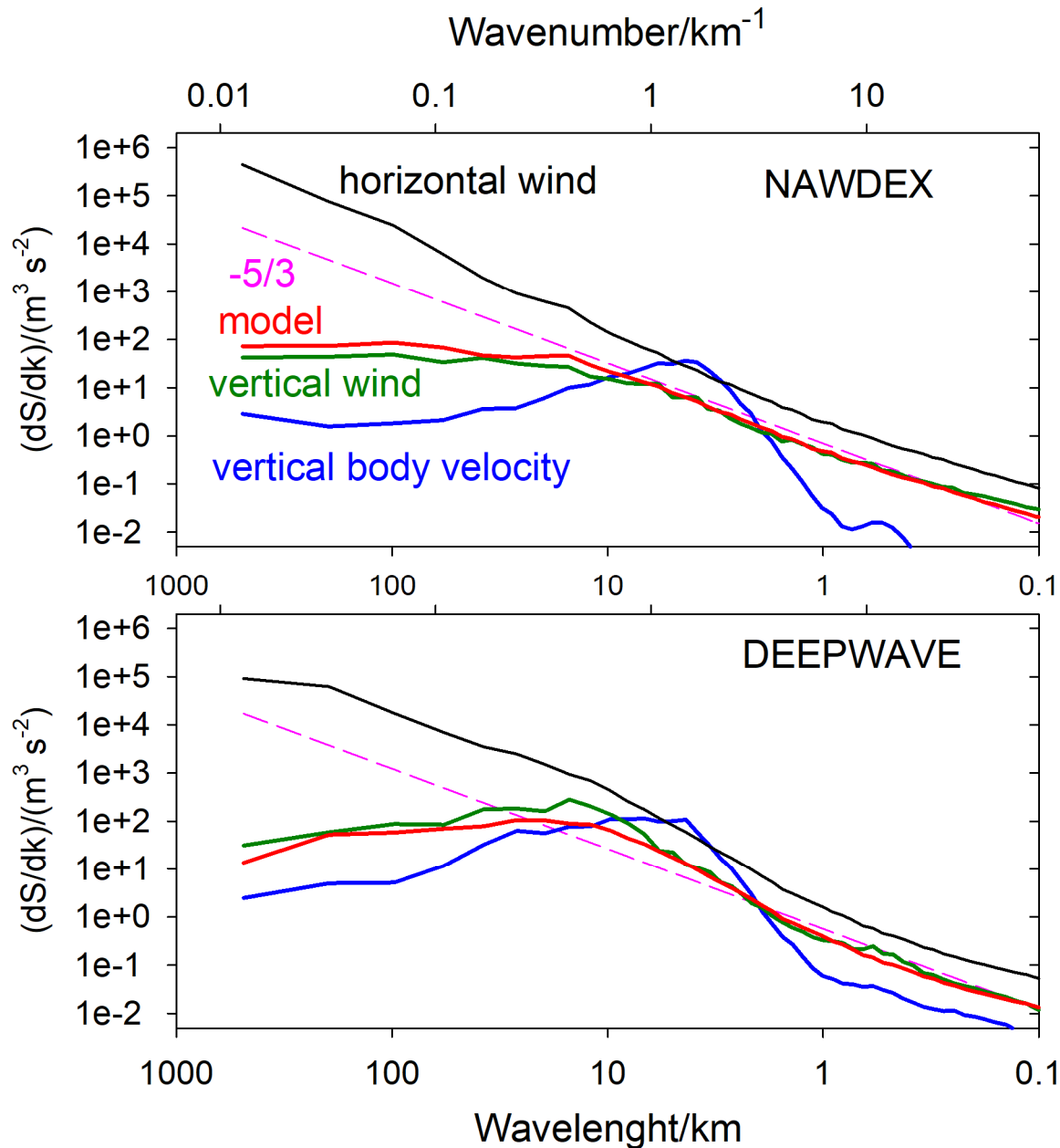
Again: Mean measured velocity spectra



How to explain
the **w** spectra?

Impact of vertical
body motions?

Mean measured and modelled velocity spectra

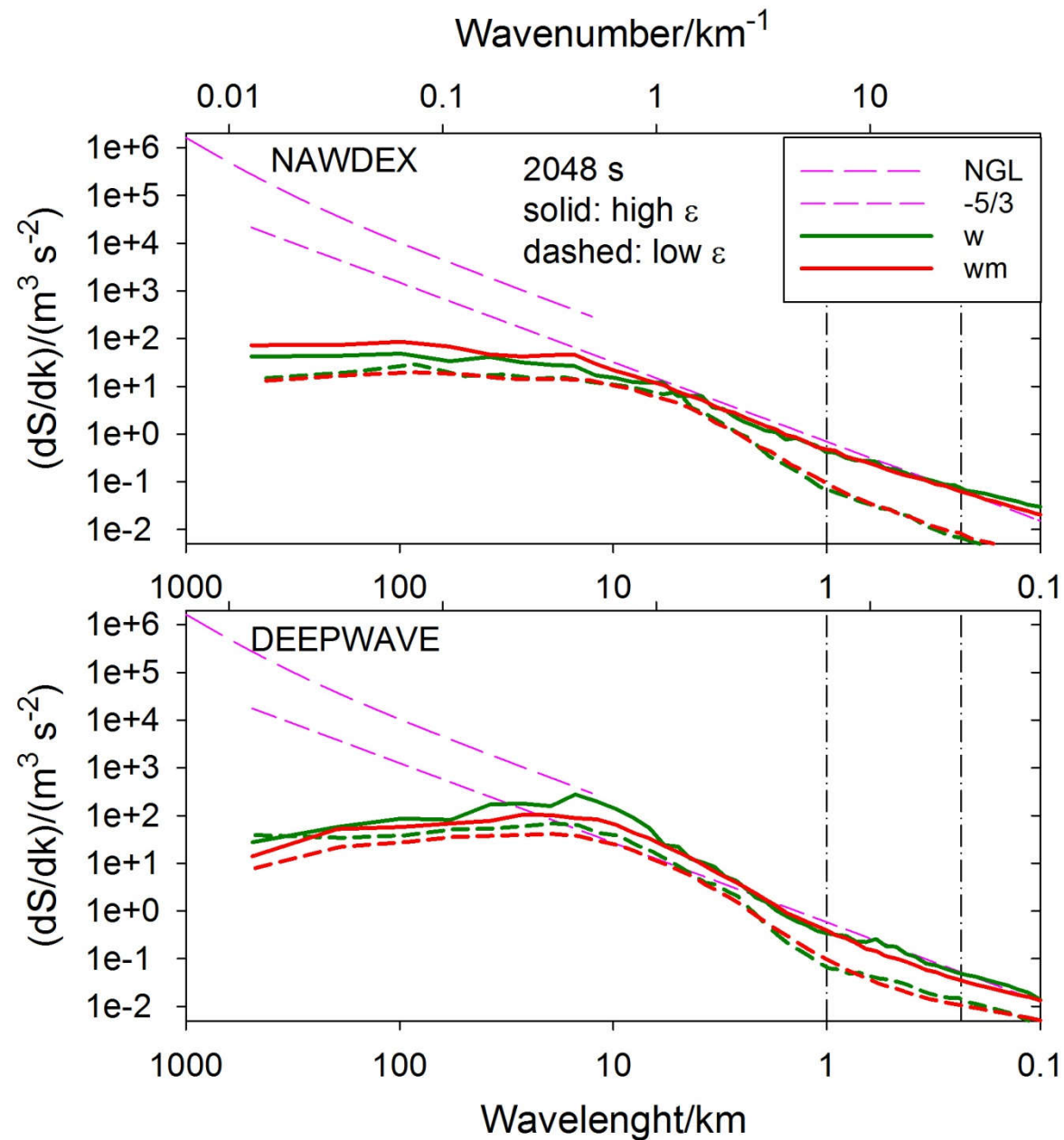


How to explain the spectra?

Impact of vertical body motions?

Model for w-spectrum

Comparison of measured and modeled w-spectra

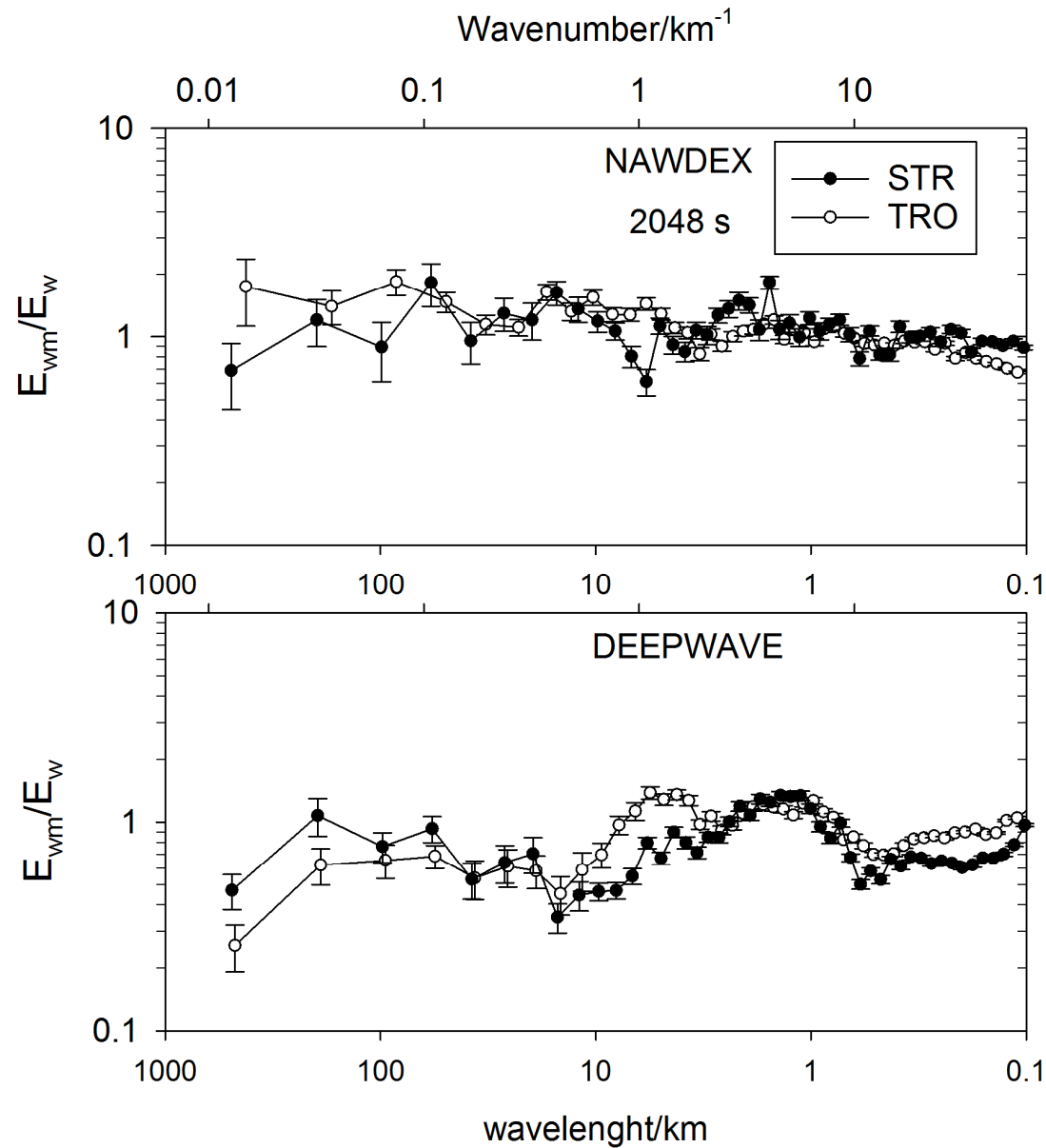


Model
and
observations

similar
at high and low ε
in both experiments

h as measured
 $d=1/2, \beta=0.11, \alpha=1/2$

Ratio of measured and modeled w-spectra

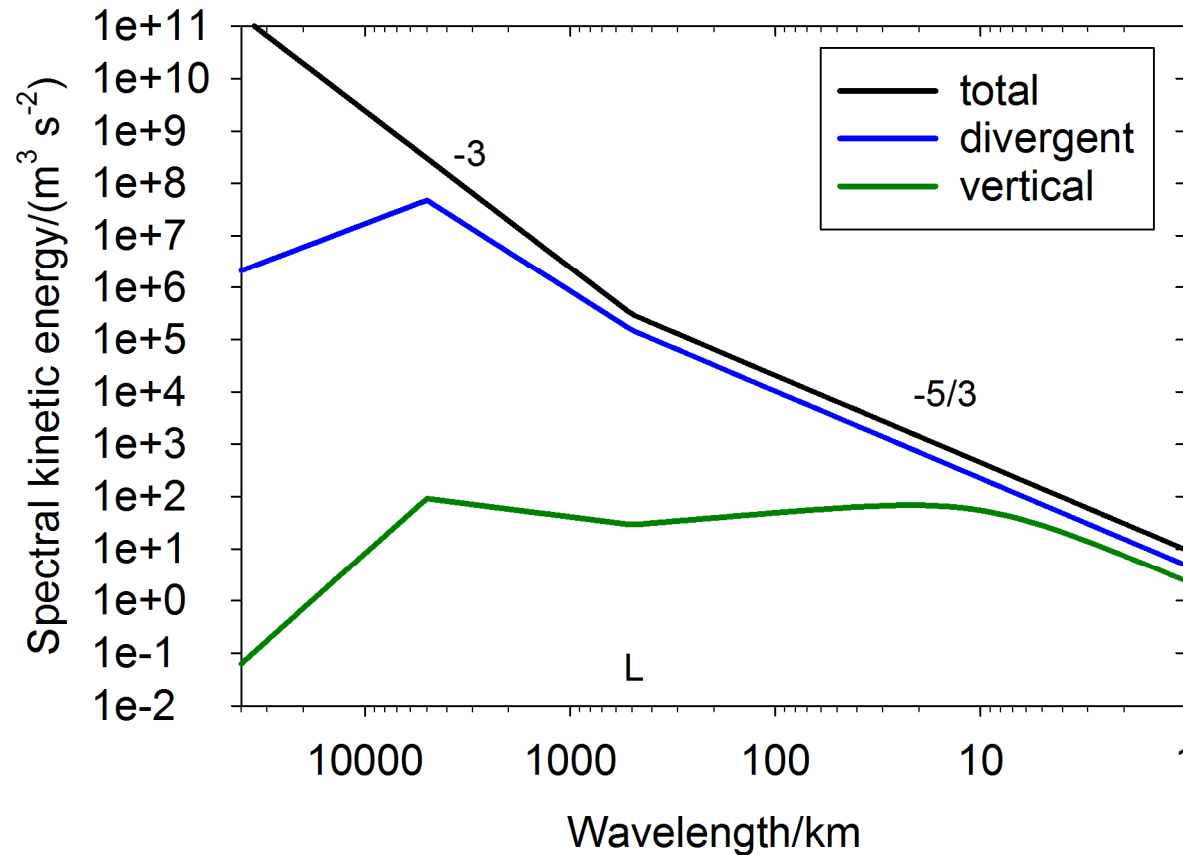


about 30 %
deviations

Implications

- Transition scale L increases for stronger w -variance
- Potential energy follows w spectrum at small scales
- The scales carrying w -variance are of order height

Schematic sketch of E_w for two transition scales L

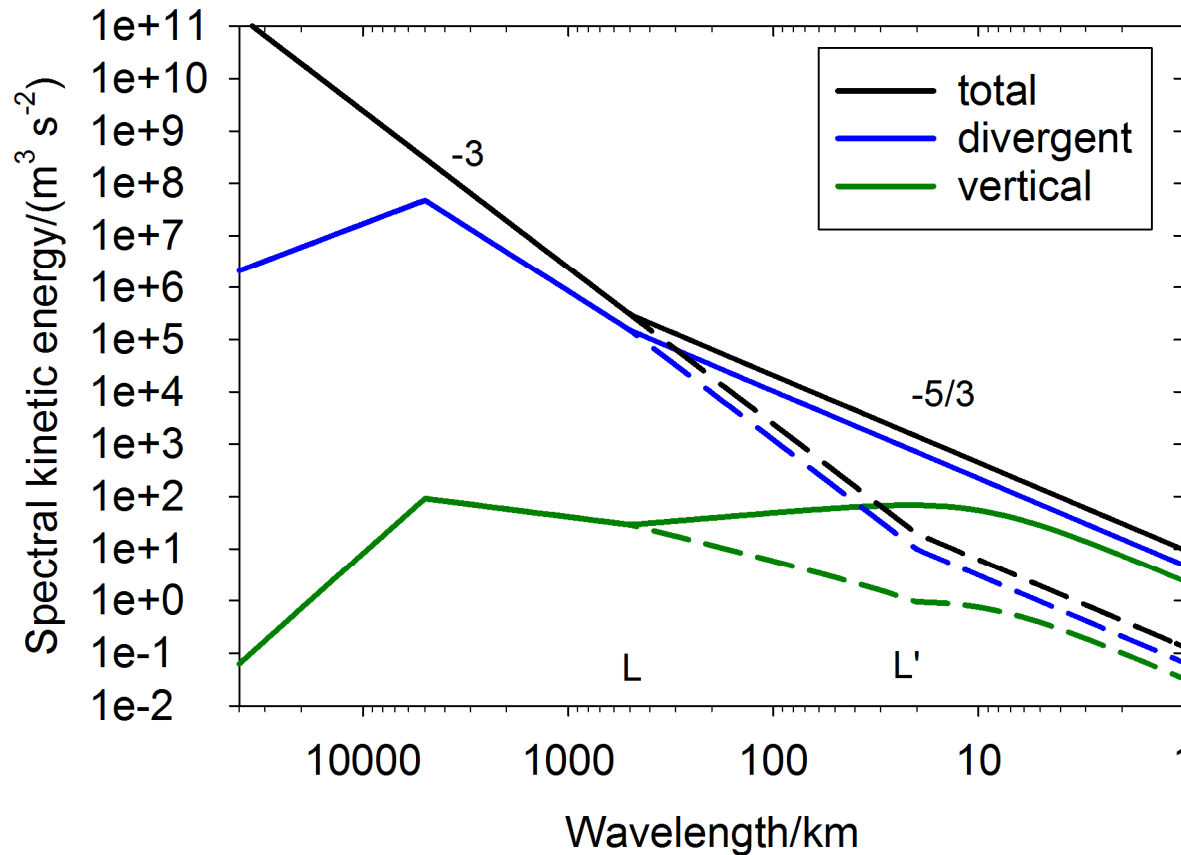


A shift in the transition scale L has strong impact on w-spectra.

This suggests dynamical importance of vertical motions for this slope transition

$$E_w(k, h) = \frac{\alpha(h_{\text{eff}} k)^2}{\alpha + (h_{\text{eff}} k)^2} E_d(k, h), \quad h_{\text{eff}} = \beta h$$

Schematic sketch of E_w for two transition scales L

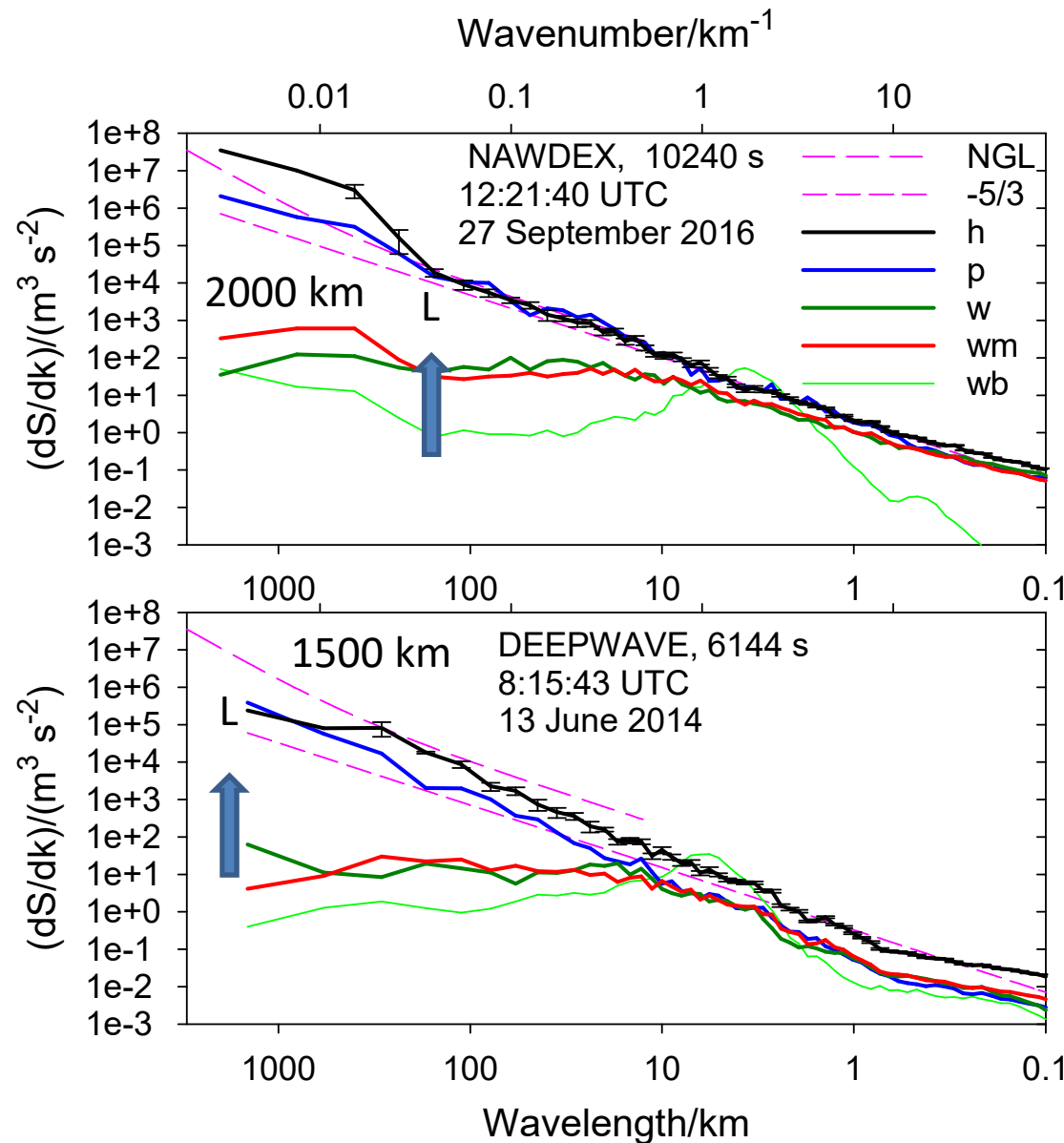


A shift in the transition scale L has strong impact on w-spectra.

This suggests dynamical importance of vertical motions for this slope transition

$$E_w(k, h) = \frac{\alpha(h_{\text{eff}} k)^2}{\alpha + (h_{\text{eff}} k)^2} E_d(k, h), \quad h_{\text{eff}} = \beta h$$

Measured and modeled w-spectra for the longest legs



$$\langle w'^2 \rangle =$$

$$0.024 \text{ m}^2 \text{ s}^{-2}$$

$$L = 200 \text{ km}$$

$$0.068 \text{ m}^2 \text{ s}^{-2} L$$

$$L > 1000 \text{ km}$$

Temperature spectra are similar to wind spectra

Spectrum of potential energy

$$E_p(k) = \frac{1}{2} \frac{g^2}{N^2 T_0^2} E_T(k)$$

$$\frac{1}{2} \frac{g^2}{N^2 T_0^2} \approx (2 \text{ to } 10) \frac{\text{m}^2}{\text{s}^2 \text{K}^2}$$

$$E_p(k) \approx E_u(k) \approx E_v(k)$$

w converts kinetic into potential energy and backward

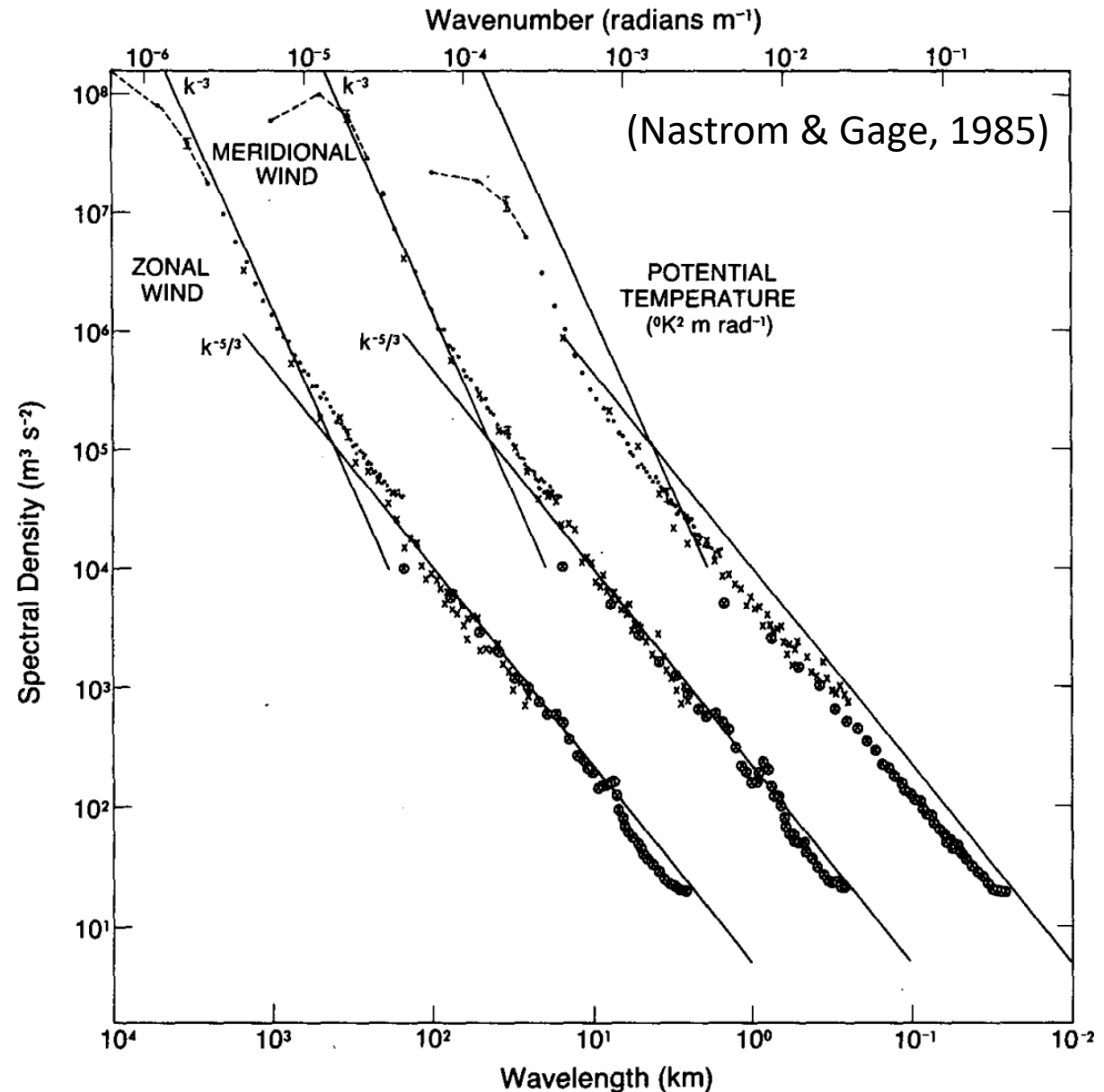
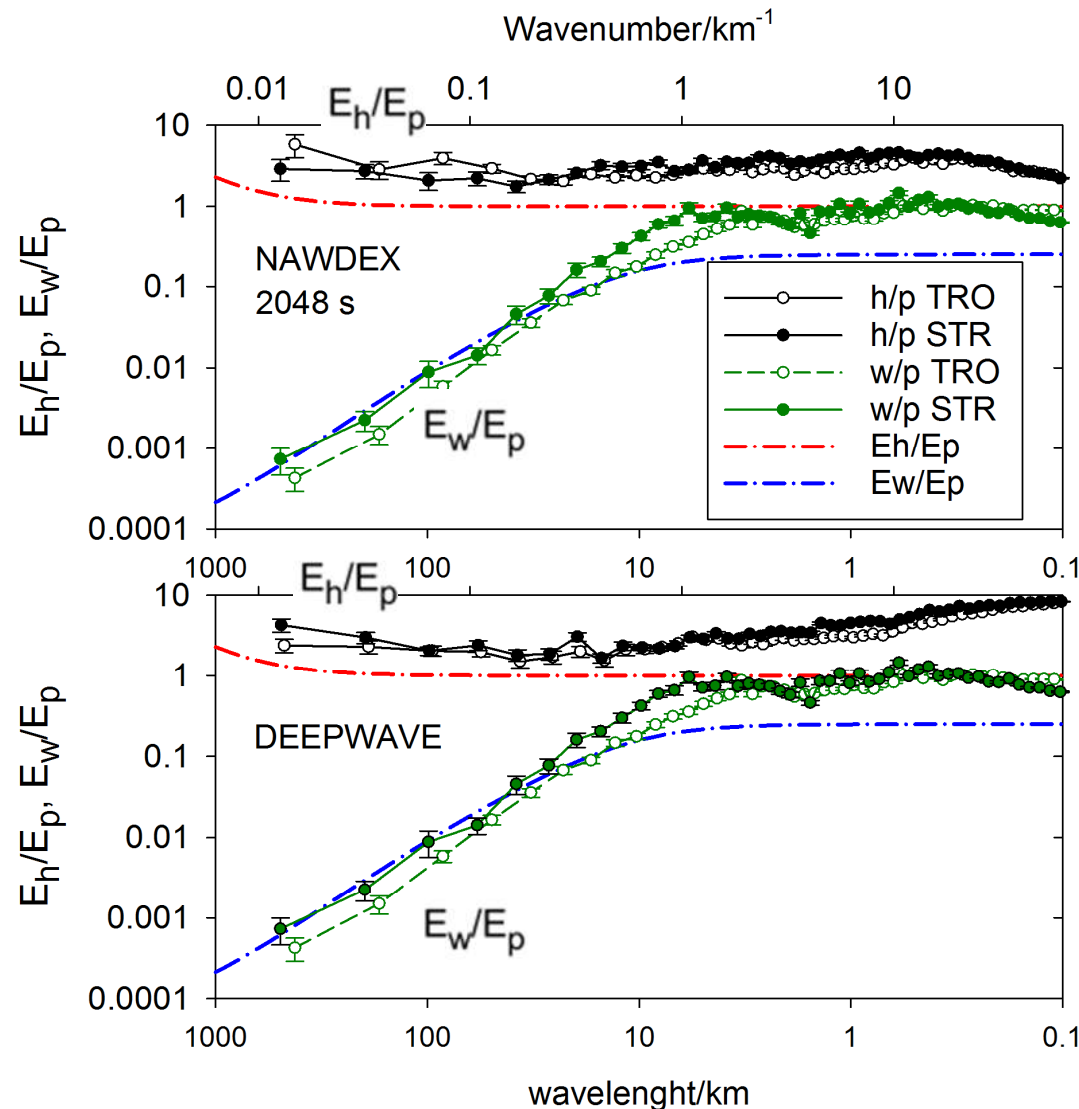


FIG. 3. Variance power spectra of wind and potential temperature near the tropopause from GASP aircraft data. The spectra for meridional wind and temperature are shifted one and two decades to the right, respectively; lines with slopes -3 and $-5/3$ are entered at the same relative coordinates for each variable for comparison.

Ratio of kinetic to potential energies

Comparisons with model spectra reflect contributions from quasi-geostrophic motions and gravity waves



Red and blue lines are models derived from linear gravity theory (e.g., Fritts and Alexander, 2003, Geller and Gong, 2010) for given E_h using our model for E_w/E_h

Consistent with gravity wave theory:

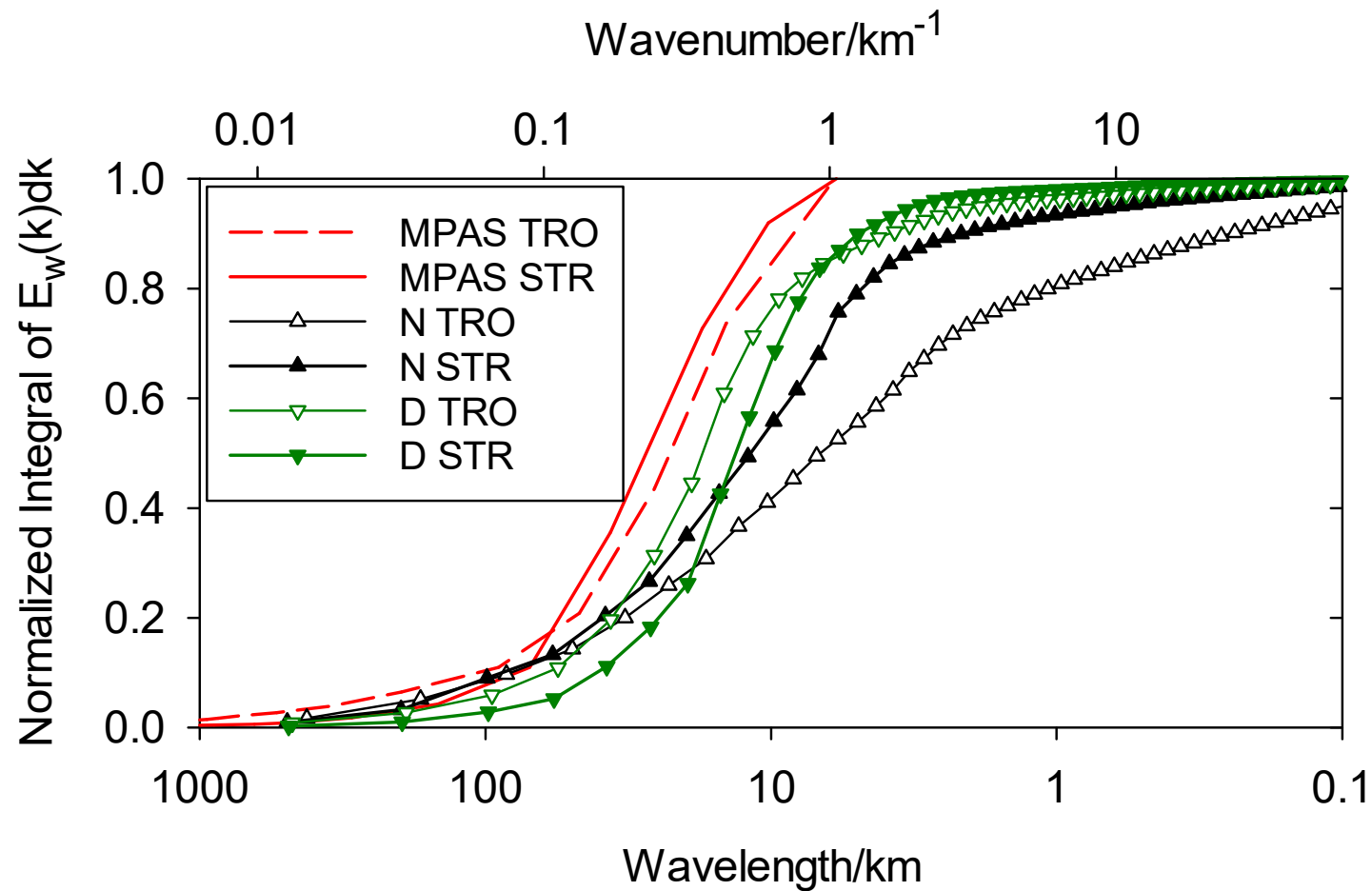
$$E_w < E_p < E_h$$

for

$$f < \omega < N$$

But gravity wave models alone underestimate E_h/E_p and E_w/E_p

Which scales contribute most to w-variance?

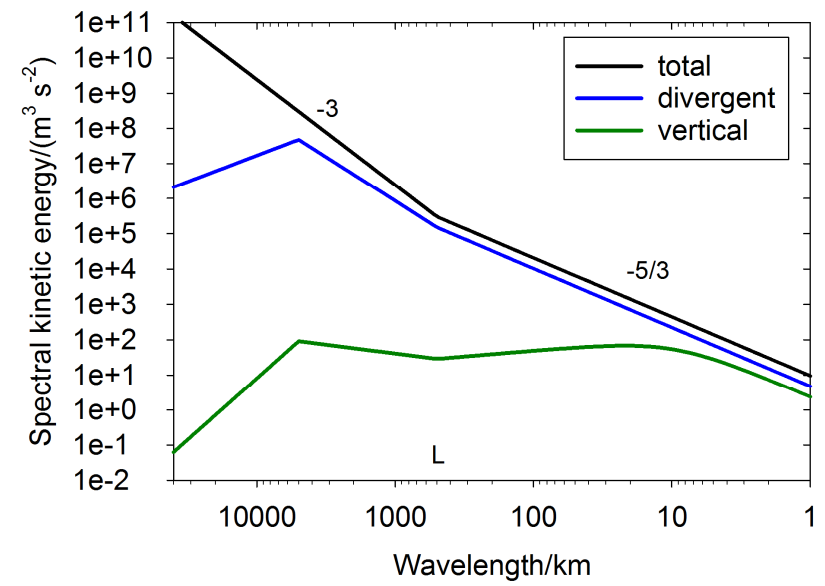


0.5 to 80 km: 90 %

7 to 17 km: 50 %

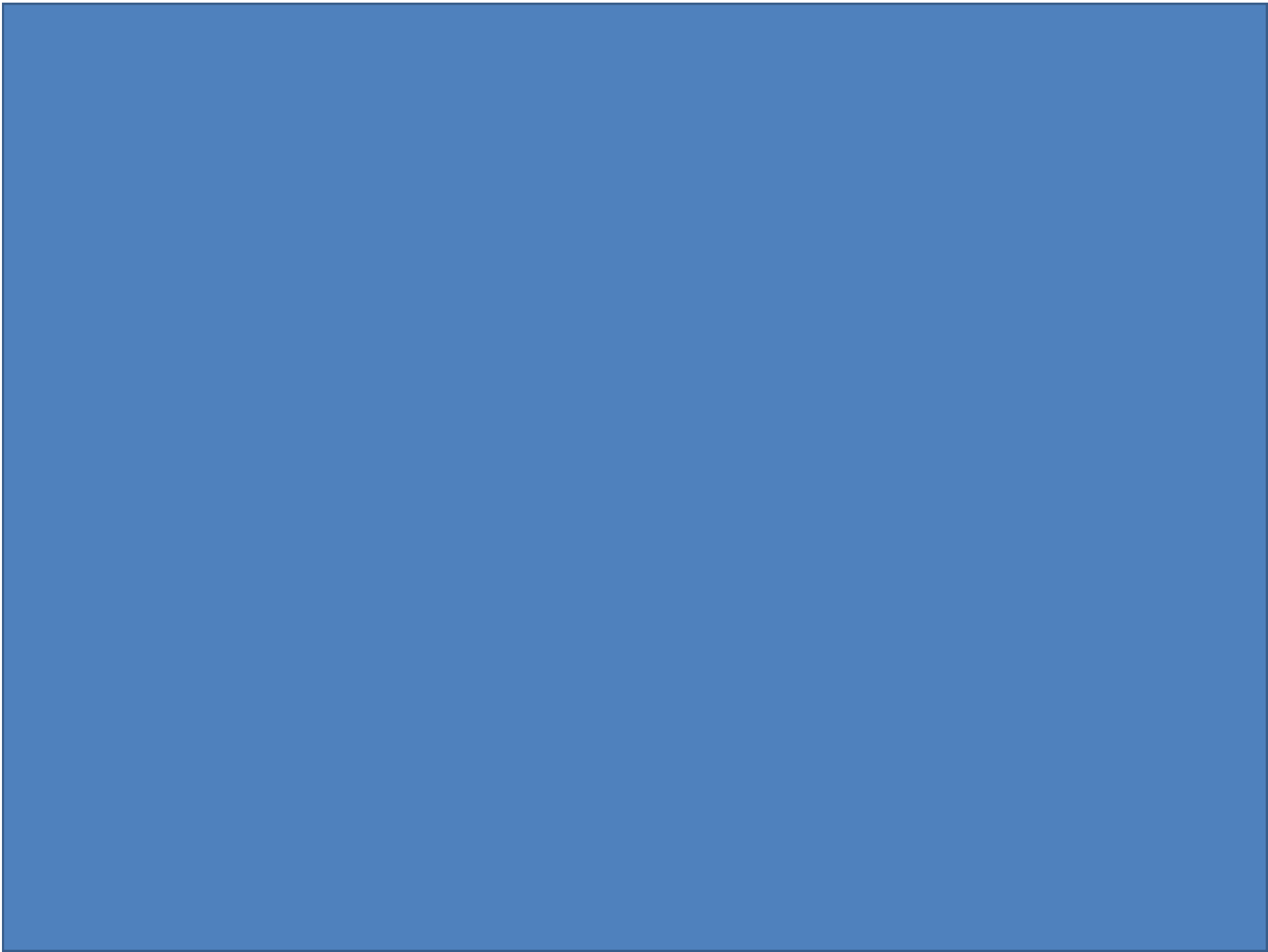
Key Points

- Spectra of vertical and divergent horizontal velocity are connected kinematically at large scales and dynamically at small scales.
- Model is consistent with global (and regional) models and flight experiments within $\sim 30\%$
- Maxima in observed vertical velocity spectra near 4 to 15 km wavelengths occur together with flat divergent horizontal spectra.
- Enhanced vertical motions shift the transition scale L between the -3 and a flatter ($\sim -5/3$) spectrum in the canonical spectrum to larger scales.



Enjoy
(e)motions





Measured velocity spectra, mean over all legs

